ACS Infectious Diseases

Review

Ten years with NDM-1 metallo #-lactamase: from structural insights to inhibitor design.

Pasquale Linciano, Laura Cendron, Eleonora Gianquinto, Francesca Spyrakis, and Donatella Tondi

ACS Infect. Dis., **Just Accepted Manuscript** • DOI: 10.1021/acsinfecdis.8b00247 • Publication Date (Web): 13 Nov 2018

Just Accepted

ACS Publications

is published by the American Chemical Society. 1155 Sixteenth Street N.W., Washington, DC 20036

Ten years with NDM-1 metallo β-lactamase: from structural insights to inhibitor design.

Pasquale Linciano[1]; Laura Cendron[2]; Eleonora Gianquinto[3]; Francesca Spyrakis[3]; Donatella Tondi[1]*

[1]Department of Life Sciences, University of Modena and Reggio Emilia, Via Campi 103, 41125, Modena, Italy; [2]Department of Biology, University of Padova, Viale G. Colombo 3, 35131 Padova, Italy; [3]Department of Drug Science and Technology, University of Turin, Via Pietro Giuria 9, 10125, Turin, Italy

Corresponding author: Donatella Tondi; *donatella.tondi@unimore.it*

The worldwide emergence of metallo β-lactamase NDM-1 as carbapenemase able to hydrolyze near all available β-lactam antibiotics has characterized the last decade, endangering efficacious antibacterial treatments. No inhibitors for NDM-1 are available in therapy, nor promising compounds are in the pipeline for future NDM-1 inhibitors.

We report the studies dedicated to the design and development of effective NDM-1 inhibitors. The discussion for each agent moves from the employed design strategy to the ability of the identified inhibitor to synergize β-lactam antibiotics. A structural analysis of NDM-1 mechanism of action based on selected X-ray complexes is also reported: the intrinsic flexibility of the binding site and the comparison between penicillins/cephalosporins and carbapenems mechanisms of hydrolysis are evaluated.

Despite the valuable progresses in terms of structural and mechanistic information, the design of a potent NDM-1 inhibitor to be introduced in therapy remains challenging. Certainly, only the deep knowledge of NDM-1 architecture and of the variable mechanism of action that NDM-1 employs against different classes of substrates could orient a successful drug discovery campaign.

Keywords: NDM-1 Metallo β-lactamase; structure-based drug design; enzyme inhibitors, biological activity, bacterial resistance, structural analysis.

Bacteria multidrug resistance poses a real menace to public health, calling for new discoveries and innovation in antibiotic research.[1,2] In Enterobacteriaceae, drug resistance is mainly attributed to the expression of a large number of diverse β-lactamases (BLs), enzymes able to hydrolyze β-lactam antibacterials. Several drug design campaigns led, so far, to the development of β-lactam drugs resistant to BLs (i.e., methicillin, last generation cephalosporins, and carbapenems) and to the design of BLs inhibitors to be co-administered with β-lactam antibacterials, thus protecting them from BLs hydrolysis.[3] However bacteria promptly reply to last developed antimicrobials *via* the production of BLs with broader spectrum of action, leaving few alternatives for the treatment of resistant infections.[4,5] In particular carbapenemases, BLs able to hydrolyze even the last resort antibiotics (i.e. carbapenems) are rapidly disseminating worldwide.[6]

According to Ambler's classification,[7,8] BLs are categorized in class A, B, C and D, with classes A, C and D being serine BLs (SBLs) (e.g., KPC, AmpC and OXA enzymes),[9–11] and class B being metallo BLs (MBLs) (e.g., VIM, IMP, NDM).[12] Among them, class B carbapenemases are the most worrisome, since they catalyze the hydrolysis of nearly all available β-lactam antibiotics.[13,14] Despite the enormous research effort to design effective drugs to counteract their extensive hydrolytic ability, currently no clinical inhibitor able to reverse the resistance mediated by MBLs has been approved in therapy.[15,16]

The hydrolysis performed by MBL is catalyzed by one or two zinc atoms located in the active site. Depending on the number of zinc atoms, MBLs are separated into three subclasses: B1, B2 and B3.[12,17] Among these, B1 subclass is the most clinically relevant and includes New Delhi Metallo-β-lactamase-1 (NDM-1), an enzyme that represents a serious threat to human health in light of its substrate promiscuity, broad-spectrum of action, appearance of variants and transferability.[18] Furthermore, NDM-1 is characterize by a unique cellular localization conferring to the protein higher stability to adverse condition like Zn depletion.[19]

Since its discovery in 2008,[20] NDM-1 has experienced the fastest and widest geographical spread among MBLs and bacterial infections harbouring plasmid-encoded NDM-1 have rapidly emerged worldwide.[1,6,21] NDM-1 production confers resistance to all β-lactam antibiotics, with the only exception of monobactams (i.e. aztreonam).[22] However, monobactams can be inactivated by many SBLs normally co-produced with NDM-1, thus expanding bacteria resistance.[23] Resistance genes encoding for MBLs are rapidly spread through plasmids and have also been reported to be located on gene cassettes, further facilitating the horizontal transmission to other microorganisms.[24,25] Nevertheless, plasmids carrying NDM-1 genes are often associated with additional resistance markers encoding other antibiotic-resistance mechanisms, including those for quinolones, aminoglycosides, rifampicin, chloramphenicol, and macrolides.[26–29] As a consequence, clinical strains producing

NDM-1 are only susceptible to last line antibacterial agents, e.g. colistin, tigecycline or fosfomycin, which all have toxicity limitations.[30]

Structure and catalytic activity of NDM-1

Structurally, NDM-1 belongs to the subclass B1 of MBL family, characterized by a distinctive αβ/βα sandwich fold. The active site, delimited by flexible loops (loop 3 and 10), contains two divalent zinc ions bridged by a hydroxide ion (**Figure 1A**). The first zinc ion (Zn1) is coordinated by His120, His122, His189 and the bridging hydroxide, corresponding to w1 (**Figure 1B**), whereas the second zinc ion (Zn2) is coordinated by Asp124, Cys208 and His250. Moreover, an apical water molecule (w2) is in close proximity, as reported (**Figure 1B**; numbering as from UNIPROT and NDM-1 X-ray structures on pdb).[31–34] In the binding site, Zn1 orientates the carbonyl group of the substrate for the nucleophilic attack to occur, while Zn2 interacts with the amide nitrogen and the carboxyl group, characteristics of β-lactam antibiotics. The aforementioned hydroxide is responsible for the nucleophilic attack performed on β-lactam rings, eventually leading to substrate hydrolysis.[12]

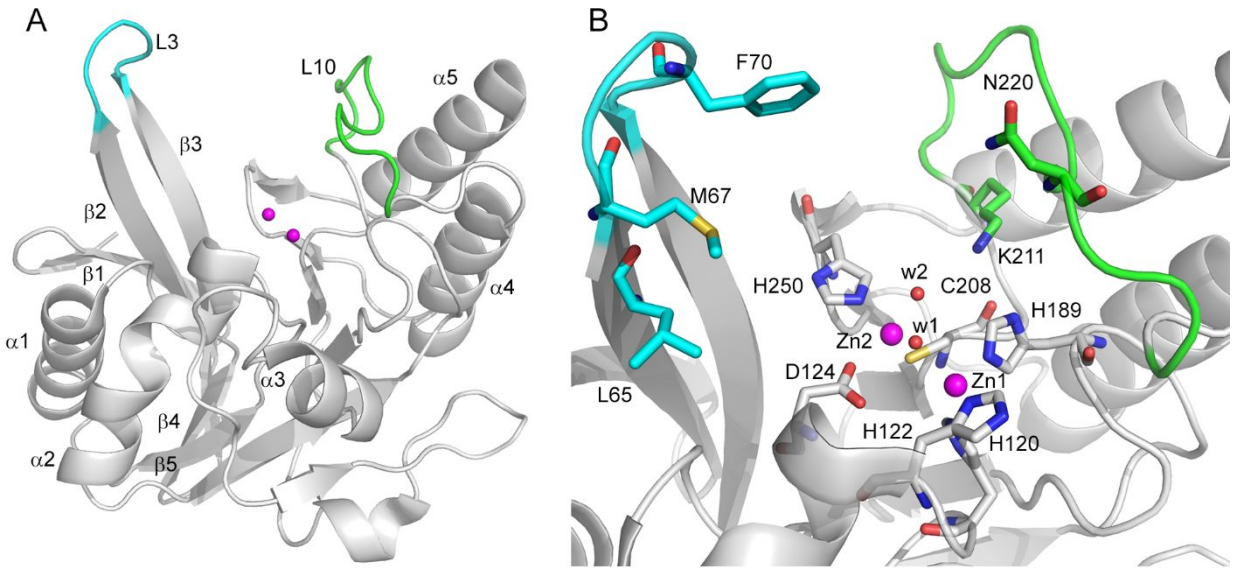

Figure 1. NDM-1 architecture. **A**) Overall protein folding. The two zinc ions are shown as magenta spheres. Loop 3 and 10 are coloured in cyan and green, respectively (PDB code 3spu).[32] The secondary structures are labelled according to Groundwater *et al*. and Kim *et al*.[22,33] **B**) Inset of the active site. Critical residues and waters referred in the text are labelled. The figure was prepared with Pymol 2.1.1.

The NDM-1 active site appears quite open and surrounded by several loops. Among these, the hairpin L3 loop, involved in substrate binding recognition, is characterized by the presence of hydrophobic

residues (Leu65, Met67, Phe70 and Val73) interacting with substrate hydrophobic substituents, while the L10 loop includes residues coordinating Zn2 (Cys 208), as well as residues interacting with the substrate carboxyl group (Lys211 and Asn220).[31,32]

The hydrolytic activity of MBLs and, in particular, of NDM-1 has been largely investigated. During the catalysis, the nucleophilic hydroxide attacks the substrate carbonyl carbon, a transient adduct is formed and stabilized through Zn interactions, resulting in the C-N bond cleavage **(Figure 2)**.[12,35,36] After the dissociation of the product from the active site and the regeneration of the bridging hydroxide, the enzyme is reactivated for a new hydrolytic reaction **(Figure 2)**. Over the years, numerous studies on this mechanism of action have been conducted and a few variants have been described.[17,21,31,35,37–39] Particular attention has been paid to the formation of one or two transition states, to the identity of the nucleophile, to the proton donor necessary to neutralize the β-lactam amide nitrogen, as well as to the substrate binding mode (see the paragraph "Structural insights on NDM-1 active site").[31,35,37,38,40] The reaction, proceeding through the formation of a stabilized anionic intermediate, has been deeply investigated by enzyme kinetics, X-ray evidences and NMR studies on cephalosporin intermediates. The protonation of this anionic intermediate represents the rate limiting step of the overall process.[41–43] However the nature of the proton donor still remains a controversial aspect.[44–46] This and other mechanistic features of NDM-1 still need a better clarification.

Recently, NDM-1 X-ray structures in complex with intermediates and products of hydrolysis of imipenem (IPM) and meropenem (MEM) were released, strongly suggesting a distinct mechanism for carbapenem hydrolysis, with respect to that described for penicillins and cephalosporins.[47] As reported by Feng *et al*., the hydrolysis of carbapenems by NDM-1 presents several peculiar aspects (**Figure 3**). First, the negative charge on pyrroline ring, consequent to the hydrolysis of the β-lactam ring, is delocalized over a conjugate π-system in an equilibrium between the two intermediate EI_1 and EI_2. The absence of the bridging water, necessary for the protonation of the pyrroline nitrogen, favours the shift of the equilibrium toward the intermediate EI_2, which could undergo two different pathways for the product release. EI_2 could be protonated on C2 to give EI_3 that evolves to EP. Alternatively, EI_2 could shift to a conformation observed in EP', before undergoing protonation (EP). Moreover, the absence of the bridging water affects the rate-limiting step of intermediate protonation. Proton uptake comes from a solvent molecule entering the pocket from the exterior space, justifying the exclusive attack of the proton in the beta position on the pyrroline ring of the carbapenem intermediate.[36]

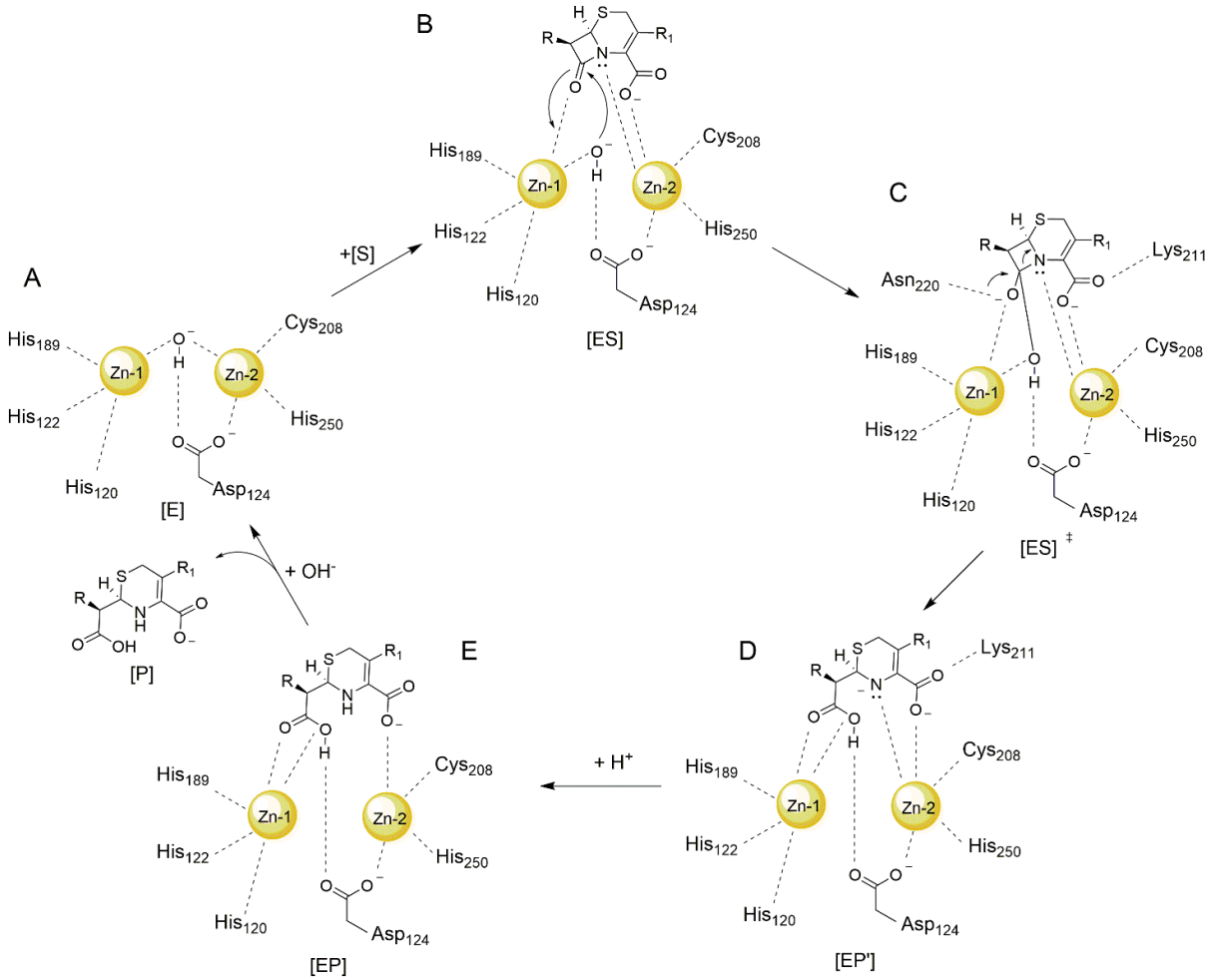

Figure 2. Hydrolytic cycle of NDM-1 on cephalosporin substrate.[36] A) NDM-1 catalytic site in its active state; B) Binding of cephalosporin substrate to the active site and nucleophilic attack of hydroxyl group to the β-lactam ring; C) tetrahedral transition state; D) binding of the cephalosporin hydrolyzed product to the NDM-1 active site; E) neutralisation of the hydrolyzed product, release of the inactivated cephalosporin and reactivation of NDM-1 catalytic site in its active state.

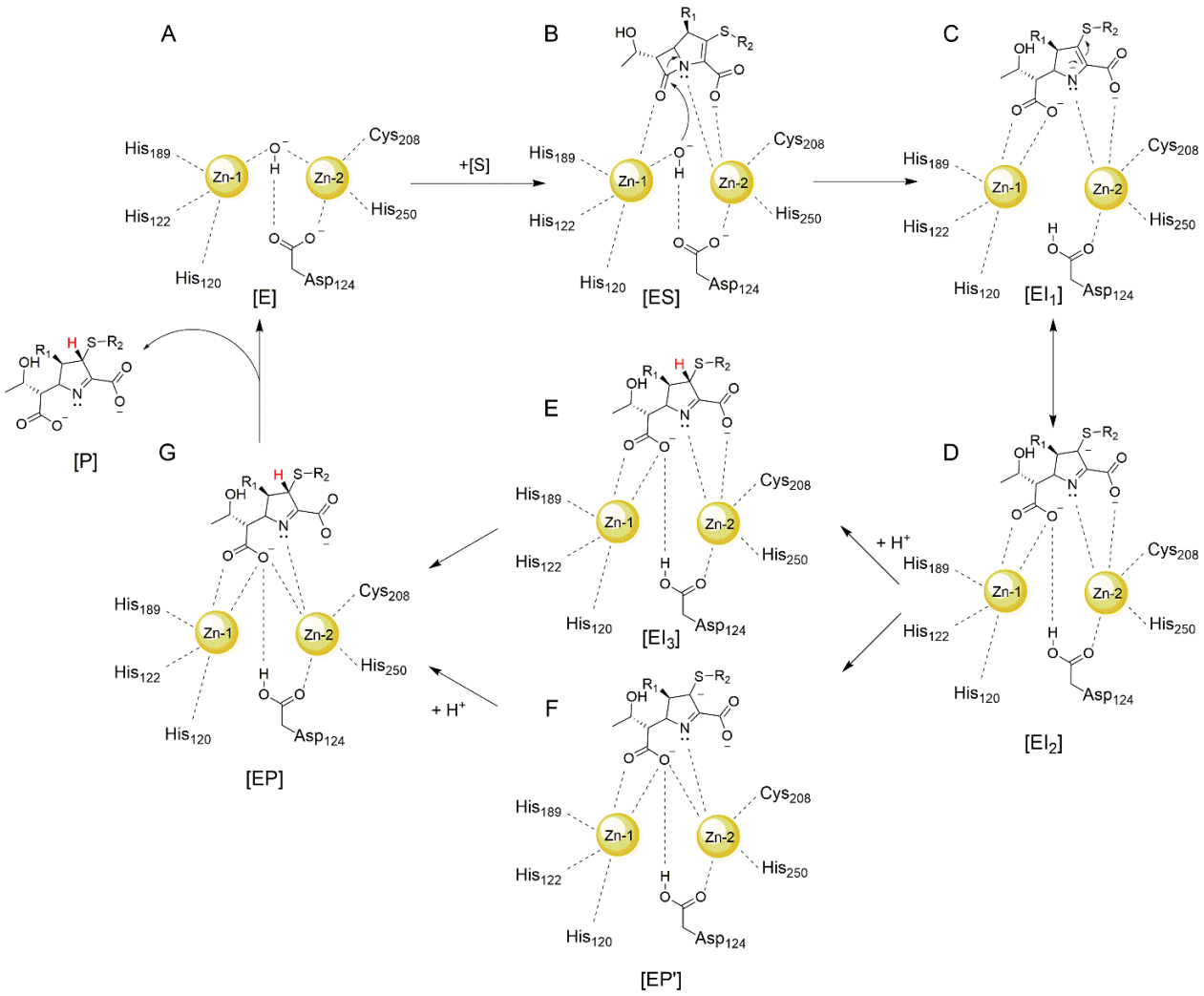

Figure 3. Hydrolytic cycle of NDM-1 on carbapenems as suggested by Feng *et al*.[47] A) NDM-1 in its active state; B) coordination of the enzyme with the carbapenem substrate and nucleophilic attack of hydroxyl to the β-lactam ring; C, D) delocalization of the negative charge on the pyrroline ring; E) protonation at C-3 to give intermediate IE_3; F) shift to configuration EP'; G) coordination of the final hydrolysis product to NDM-1, release of the product P and regeneration of the enzyme in its active state.

In addition, Lisa *et al*., recently reported a fully biochemical and biophysical study of IPM hydrolysis by bi-Zn(II) B1 enzyme (i.e. NDM-1 and BcII) and the mono-Zn(II) B2 and B3 BLs.[35] In particular, focusing on the hydrolysis of IPM (**Figure 4**), they proposed the binding of the substrate to Zn2 by means of the carboxylate group at C3 and the simultaneous detachment of the hydroxide to generate a potent nucleophile (**Figure 4**, state **B**).

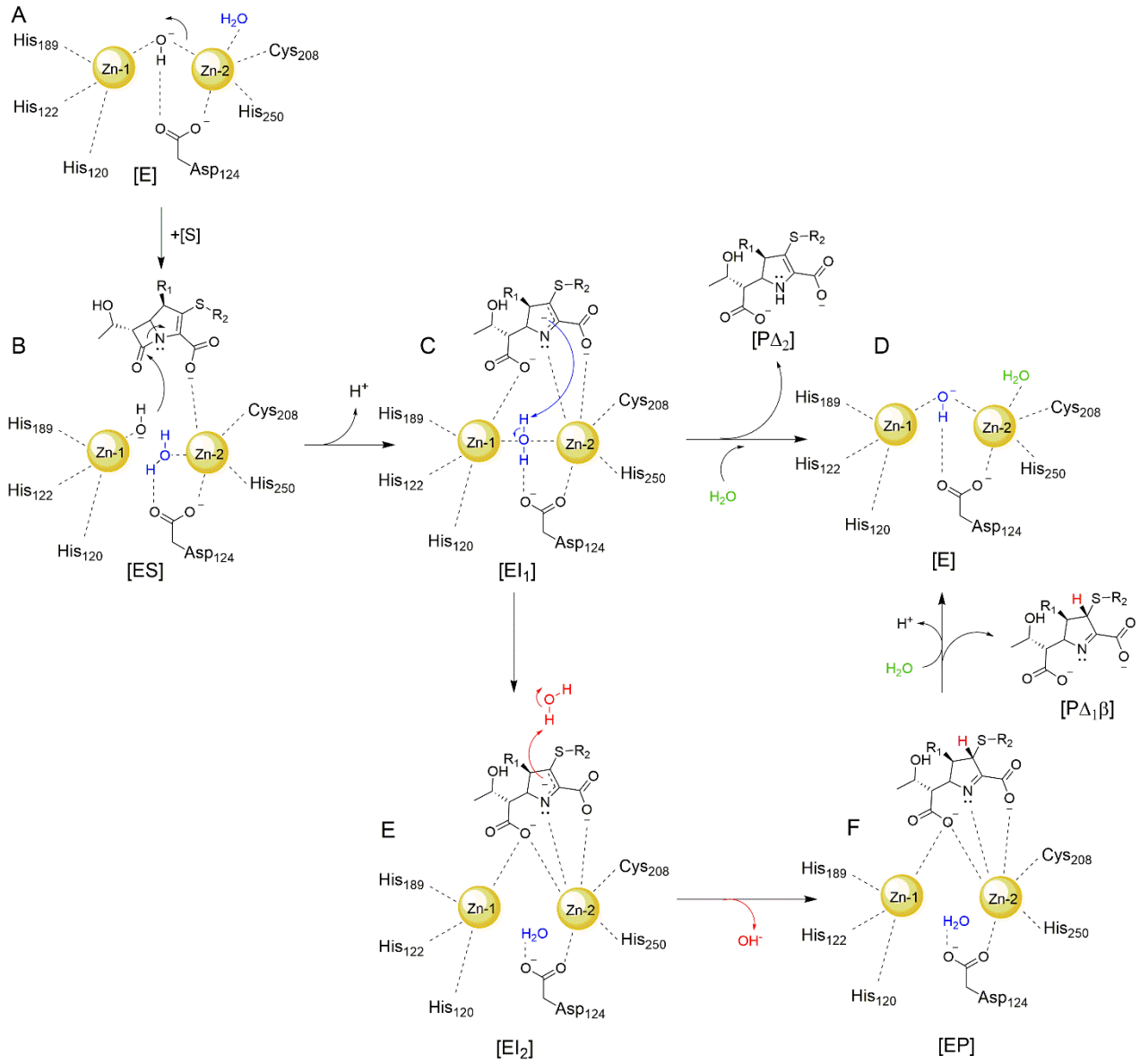

Figure 4. Hydrolytic cycle of bi-Zn(II)-MBLs (including NDM-1) on carbapenem as suggested by Lisa *et al.*[35] A) NDM-1 in its active state; B) binding of the substrate to Zn ions and simultaneous detachment of the hydroxide to generate the nucleophile attacking the β-lactam ring; C) protonation of the anion by means of the water molecule; D) release of the product, coordination with a water molecule and regeneration of the enzyme in the active state; E) interconversion of EI_1 to the intermediate EI_2 and protonation by means of an external water molecule; F) hydrolyzed product-enzyme coordination before product release. After the dissociation of the hydrolyzed product, a second water molecule regenerates the enzyme.

In this way the hydroxide is able to attack the β-lactam ring generating the adduct EI_1 (**Figure** , state **C**). In EI_1, the deprotonated hydrolyzed-carbapenem binds to Zn1 via the carboxylate at C7 and to Zn2 through the carboxylate at C3 and through the pyrroline ring. Subsequently, the protonation by means of a water molecule elicits the hydrolyzed product, regenerating the enzyme in its active state

(**Figure** , state **D**). Alternatively, the EI_1 can interconvert to an intermediate configuration EI_2 where the carboxylate group at C7 becomes a bridging ligand coordinating Zn2 (**Figure** , state **E**). The protonation at C2 in EI_2 by means of an external water molecule leads to the EP complex lacking a metal-bound water (**Figure** , state **F**). After the dissociation of the hydrolyzed product, a second water molecule finally regenerates the enzyme in its active state (**Figure 4**, state **D**).[35]

Structural insights on NDM-1 active site

In the last years, many efforts have been made to get structural insights on NDM-1, to clarify the mechanism of action and to identify the residues that interact with the substrates and that could be targeted in drug design campaigns. At the time of writing this review, fifty structures were available in the Protein Data Bank (PDB), twenty-two of them in the apo form and the remaining twenty-eight complexed with β-lactam based substrates or product and only two with novel inhibitors (Table S1). Among substrates, we can recognize two main groups: penicillins/cephalosporins and carbapenems. In **Figure 5** the hydrolyzed forms of methillicin (A), cefuroxime (B) and IPM (C) within NDM-1 active site are reported.[21,36,47]

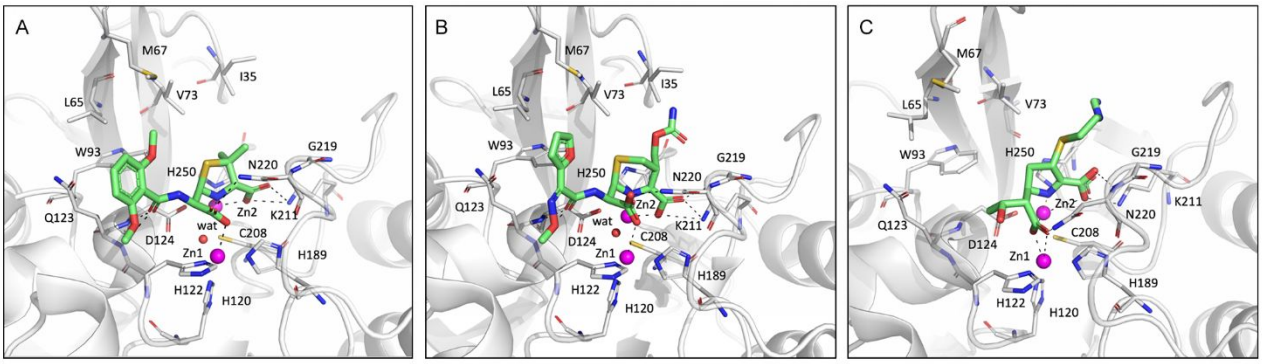

Figure 5. Close-up of hydrolyzed methicillin (A), cefuroxime (B) and IPM (C) in NDM-1 catalytic site (PDB code 4ey2,[21] 4rl0[36] and 5ypl[47], respectively). The ligands are represented as green capped sticks, the binding site residues as grey capped sticks, the zinc ions are shown as magenta spheres, the water molecule as a red smaller sphere. The hydrogen and coordination bonds are represented in black dashed lines. The figures were prepared using Pymol 2.1.1.

Apart from the different substituents, the three molecules occupy, in general, the same position in the protein binding site. Nevertheless, small differences can be observed when comparing methicillin and cefuroxime with IPM.

The hydrolysis mediated by the nucleophile hydroxide (see **Figure 2** and **Figure 3**) generates the C6-carboxylate, which intercalates the two zinc ions and establishes polar contacts with the surrounding residues. In the case of methicillin and cefuroxime, this group coordinates only Zn1 and forms a hydrogen bond with Asn220 (**Figure 5A** and **Figure 5B**). The C3-carboxylate contacts Zn2, Lys211 and Gly219. The lactam nitrogen also coordinates Zn2. Additional hydrogen bonds are formed by the methyloxy-phenylcarbonyl-amino moiety in methicillin and by the methoxy-iminoacetyl-amino moiety in cefuroxime with Gln123 and Asp124. Hydrophobic contacts with Leu65, Val73 and Trp93 further stabilize the complexes. In both cases, a water molecule is coordinated by the two zinc ions and it is hydrogen bonded by Asp124. In the case of cefuroxime, according to what reported by Feng *et al.*,[36] the carbon in position 3, bearing the R_2 group, is negatively charged and assumes a sp^3 configuration. This anionic intermediate (EI state) differs from that proposed for penicillin hydrolysis, where the negative charge is generally located on the lactam nitrogen.[48] It should be considered that the presence of a conjugated π-system could allow the rearrangement of the double bond from position 3-4 to 4-5.[36] The isolation of this cephalosporate intermediate further supports the hypothesis that the subsequent protonation represents the rate-limiting step in the hydrolytic process.

The water molecule intercalating the two zinc ions, previously mentioned, could represent the proton donor. It has been hypothesized that this water could be originally bound to Zn2 or that it could come from the solvent.[47] Interestingly, the same water is absent in the NDM-1-IPM complex (**Figure 5C**). With respect to methicillin and cefuroxime, IPM presents quite similar contacts for the β-lactam core. The newly generated C6-carboxylate hydrogen bonds Asn220 and coordinates both Zn1 and Zn2. Differently from hydrolyzed penicillins and cephalosporins, in carbapenems this carboxylic group intercalates the metals, generating a hexahedral coordinated Zn2. At the same time, the distance between Zn2 and the C3-carboxylate increases, likely destabilizing the enzyme-intermediate complex, while the lactam nitrogen still coordinates Zn2. In the present complex, Feng *et al.* also observed in addition a higher flexibility of the R_2 side-chain, which further supported the hypothesis of the complex being in the EP state, already protonated (possibly by a solvent water) and ready to leave the active site. The peculiar position of the C6-carboxylate is also responsible for the steric displacement of the mentioned water molecule that was never observed in NDM-1-carbapenemes complexes.[21,47] As also noted for methicillin and cefuroxime, the C3-carboxylate contacts Lys211 and Gly219. Very poor hydrophobic contacts are made by the hydroxyethyl moiety with Trp93.

According to these observations, the hydrolytic mechanism for penicillin/cephalosporin and carbapenem would mainly differ in the rate-limiting step of intermediate protonation, due to the different nature of the proton donor. In the absence of the bridging water, an additional water molecule has to participate to the process, possibly modifying the catalysis speed. For this reason, the structure

of the antibiotic substrate directly affects the rate-limiting step. As further support, Feng and co-workers explained the higher k_{cat} for IPM with respect to MEM (k_{cat}/K_M equal to $4.3 \cdot 10^6$ and $2.6 \cdot 10^6$ $M^{-1}s^{-1}$, respectively) with the different chemical nature of the R_2 side-chain. The IPM N-formimido group could provide a more hydrophilic environment than the MEM pyrrolidine ring, thus facilitating the entrance of a solvent molecule.[47] In this perspective, side-chains could be properly modified for the design of mechanism-based inhibitors.

Another noteworthy feature that distinguishes penicillin/cephalosporin binding mode with respect to carbapenem is the conformation of the β-hairpin L3 loop, which defines the size of the binding site groove. According to Feng *et al.,* when carbapenems are bound and hydrolyzed by NDM-1, the catalytic pocket slightly collapses with the L3 loop somehow closing the site entrance. On the contrary, when penicillins/cephalosporins are present in the pocket the L3 loop shifts backwards, allowing room for bulkier moieties (**Figure 6**). This could be likely attributed to the different extension of the R_1 side-chain, generally smaller for carbapenems.[47] The different shape and volume of the cavity in the three complexes is clearly visible in **Figure 7** with cefuroxime inducing the larger variation. The pockets were calculated by flapsite, implemented in FLAP, developed by Molecular Discovery Ltd (www.moldiscovery.com).[49,50]

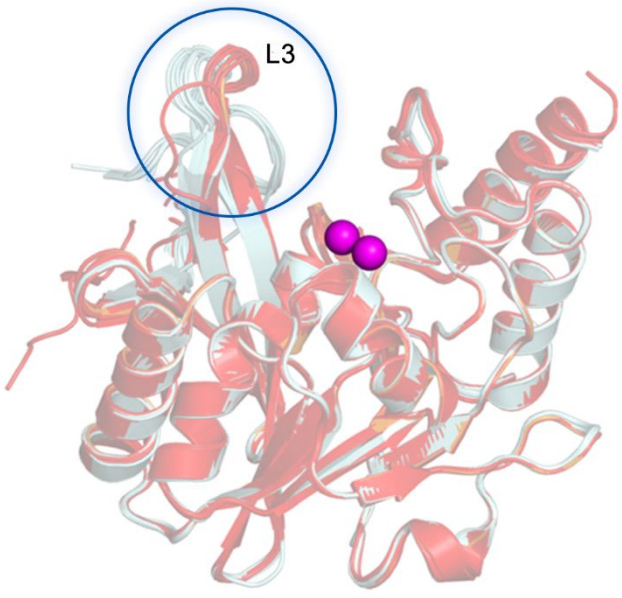

Figure 6. Superimposition of all the NDM-1 carbapenem-binding (red) and penicillin/cephalosporin (palecyan) structures reported in PDB. The L3 loop is labelled. Figures were prepared using Pymol 2.1.1.

For the three pockets, the Molecular Interaction Fields (MIFs) were also determined (**Figure 8**). In all cases the H-bond donor regions are properly filled by the two carboxylic groups. On the contrary, the hydrophobic areas are quite poorly filled, with the only exception of the methicillin methoxy group, located in a small hydrophobic contour closed to Trp93. This suggests that the design of molecules having lipophilic moieties able to form stronger hydrophobic contacts with the enzyme binding site could lead to the development of more effective inhibitors. It is also visible how the pocket MIFs for the complexes with methicillin and cefuroxime are quite similar, while some differences arise with respect to the NDM-1-IPM complex. This further supports the plasticity of the binding site and the observation that a different loop arrangement occurs when carbapenems are bound to the protein.

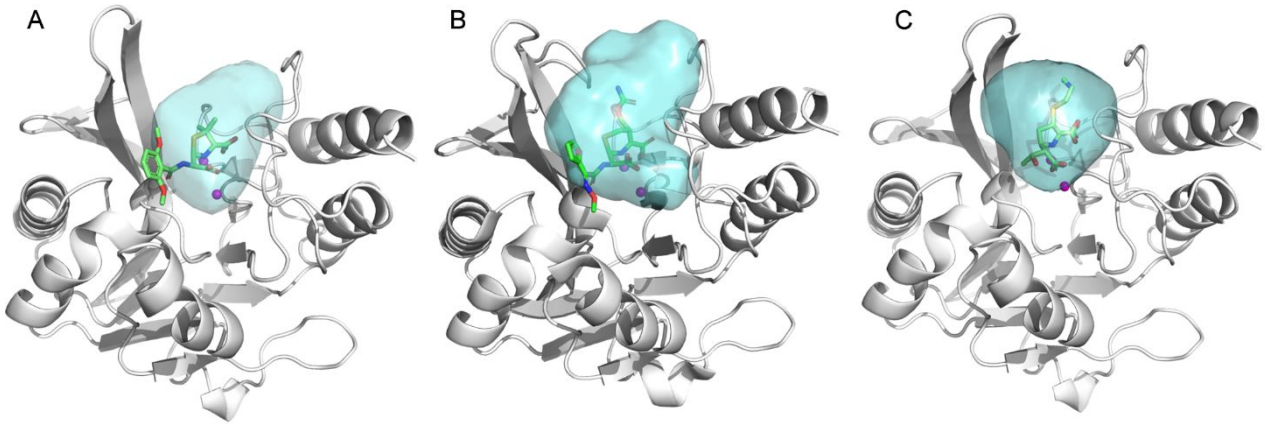

Figure 7. Pockets calculated by flapsite for NDM-1 when complexed with methicillin (A), cefuroxime (B) and IPM (C).

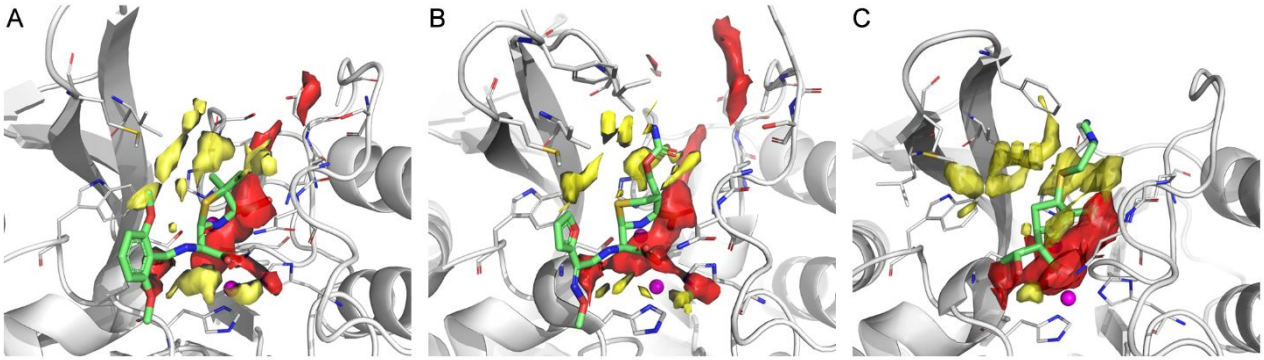

Figure 8. GRID Molecular Interaction Field calculated for the NDM-1 active site when complexed with methicillin (A), cefuroxime (B) and with IPM (C). Red contours correspond to hydrogen bond acceptor regions, yellow contours correspond to hydrophobic areas. Only residues lining the pocket have been displayed.

NDM-1 Inhibitors

While for SBLs several mechanism-based inhibitors are available in therapy and extensive structure-based drug design efforts continues to be effective,[51–58] a specific and efficacious inhibitor against NDM-1 is still missing in clinic. The lack of effective MBLs inhibitors could be mainly attributed to the structural diversity of the active sites among the three different MBLs classes, to the variability of the loop arrangement at the active site entrance and to the presence of several NDM-1 variants. In few years, indeed, NDM-1 has evolved in twenty new variants by single or double mutation at different positions, often enhancing the performance of NDM variant under low Zn(II) availability.[6,59–63]

Nevertheless, we should consider the peculiar nature of MBLs binding site which might partially interfere with the design of effective and specific inhibitors, considering that the majority of substrate-protein interactions involves the two zinc ions.[51,64] Indisputably, progresses toward a complete knowledge of the catalytic mechanism and its variability depending on the binding substrate are strictly necessary to successfully guide the rational design of clinically useful inhibitors.[12,22,35,65]

Despite the large number of molecules disclosed as NDM-1 inhibitors, only few of them were co-crystallized with the enzyme, thus limiting our knowledge about the binding mode and the mechanism of action of reported inhibitors (Table S1).[21,66]

Many excellent reviews have been published in the last years on NDM-1. Some of them are focused on the enzyme structural properties and on the mechanism of action, others on the epidemiology, spread and variants of NDM-1.[12,22,67–69]

This review is aimed to provide an exhaustive report on NDM-1 inhibitors designed and developed in the last decade. We choose to focus on novel, non β-lactam like inhibitors, with particular emphasis on the most recent advances in the field. Highlights on inhibitor design, novel chemistry and proposed mechanisms of action are discussed. The inhibitors are conveniently separated and classified in groups, according to the chemical scaffold responsible for the protein recognition. The large class of non-covalent inhibitors is mainly composed by chelating agents (EDTA, AMA, NOTA), zinc coordinating agents (mercapto aliphatic acid, thiosemicarbazones, 2-mercapto-azoles, dipicolinic acids) and boronic acid derivatives. Two smaller sections are also dedicated to covalent inhibitors and to other inhibitors not ascribable to a specific chemical class.

In order to perform a systematic study from a structural and mechanistic point of view, all the discussed compounds were analysed for their structural similarity (**Figure 9**). To our knowledge, up to now, **525** NDM-1 inhibitors have been reported in literature (*see Supporting Information*). All the inhibitors were first divided into three main groups: small molecules, natural compounds and β-lactams and further clustered, based on their main chemical scaffold and similarity. In the present

review, we will focus on a systematic description of the 17 small molecules chemical clusters identified, thus including the majority of NDM-1 inhibitors so far reported in literature. Each discussed inhibitor is identified with a progressive alphanumeric code: the number indicates the library where the inhibitor belongs to, whereas the subsequent letter uniquely identifies the molecule. The reported inhibitor activity against NDM-1 is expressed in term of micromolar IC_{50} or K_i.

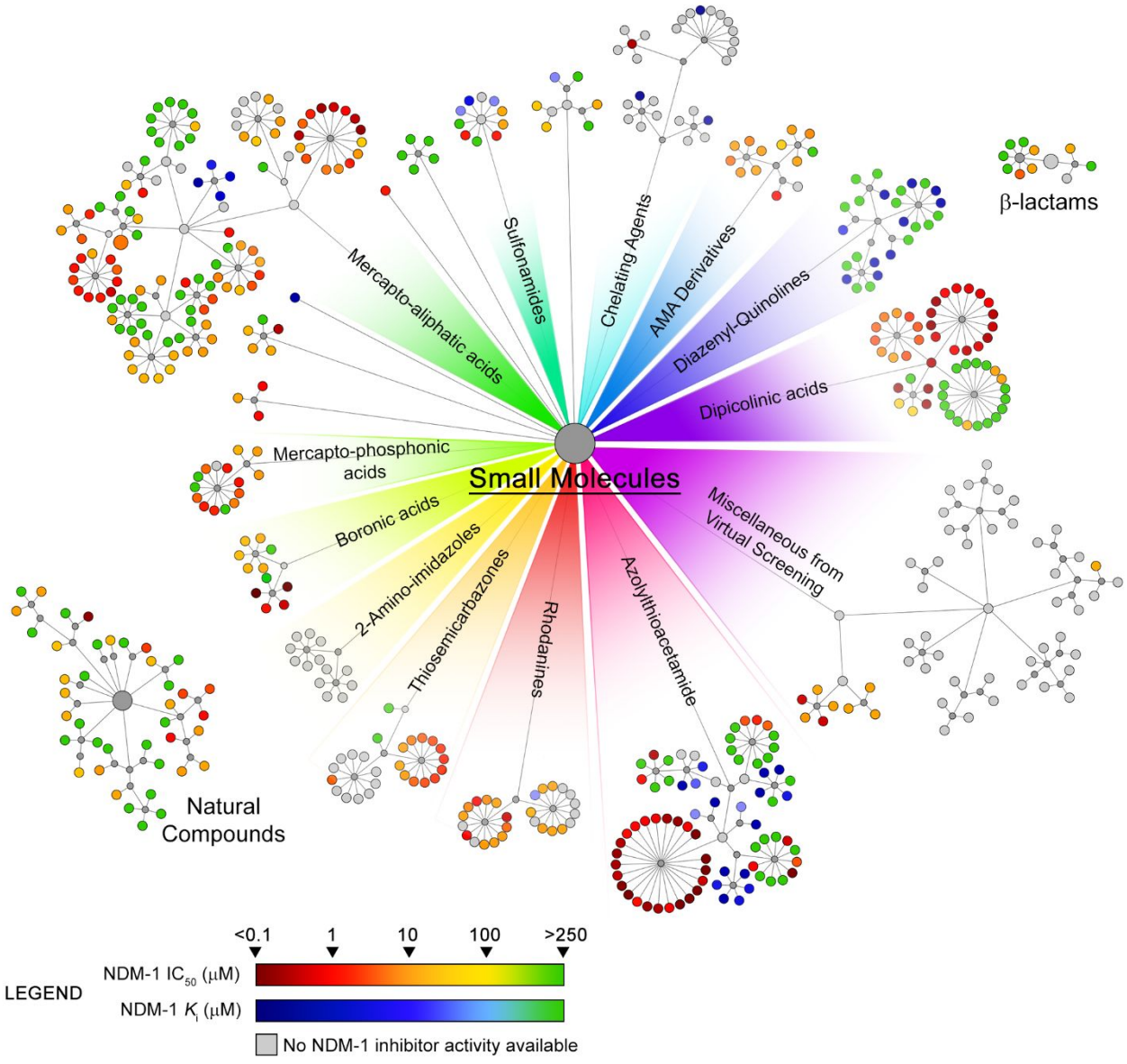

Figure 9. Dendrogram of the discussed NDM-1 inhibitors. The compounds are divided in three main groups (small molecules, natural compounds and β-lactams) and clustered according to the chemical similarity. For each molecule, the ECFP4 binary dendritic fingerprint was determined,[70] and the entire library was hierarchically clustered by Tanimoto similarity, setting a merging distance of 0.85.[71] The similarity matrix was converted with Cytoscape to the corresponding dendrogram for a more rapid and intuitive visualization.[72] In the dendrogram, each inhibitor is represented by a coloured dot at the end of each branch. Each compound is connected to the others by means of intermediate dots, closer the compounds, higher the structural similarity. All the molecules are coloured-coded according to their inhibitor activity against the enzyme, from green

to red, for IC_{50} value and from green to blue for K_i value, in micromolar (see the legend). When no activity against NDM-1 is reported, dots are coloured in grey.

Chelating agents as NDM-1 inhibitors

Molecules sequestering the zinc ions

EDTA (ethylenediamine-N,N,N',N'-tetracetic acid) is a well-known, largely used metal chelator, and its capability to potentiate other antibiotics is well documented.[73,74] Although effective, **EDTA** derivatives are non-specific and highly cytotoxic, thus preventing their clinical usage.[75] The only exception is represented by the correspondent disodium calcium salt (**Ca-EDTA**), actually approved in Japan for the treatment of lead intoxication.[76] Yoshizumi *et al*., inspired by the work of Aoki *et al*.,[77] reported that **Ca-EDTA** efficaciously potentiates the antibacterial activity of IPM and MEM in over-expressing NDM-1 *E. coli* strains. At the concentration of 32 μg/mL, **Ca-EDTA** was able to reduce the MIC of IPM and MEM down to <2 and <4 μg/mL, respectively, whereas no synergistic effects was observed in association with non β-lactams such as amikacin and ciprofloxacin. The reported effect is attributed to the capability of **Ca-EDTA** to chelate the NDM-1 active site zinc ions, thus blocking the enzyme and protecting the co-administered antibiotic from hydrolysis. Moreover, the association of IPM/cilastin with **Ca-EDTA** was able to reduce the bacteria burden of one order of magnitude in the liver of neutropenic murine model of sepsis, suggesting that the tested combination could be employed in infections mediated by NDM-1over-expressing bacteria.[78]

Recently, during a phenotypic screening of 500 natural extracts against an *E. coli* strain carrying *bla*NDM-1, Aspergillomarasmine A (**AMA)** was identified to restore MEM activity (**Figure 10**). **AMA** is a molecule that was first identified from a strain of *Aspergillus flavus oryzae* and characterized for its necrotic activity on plant leaves[79] and later re-evaluated as an inhibitor of angiotensin-converting enzyme (ACE).[80] In recent years, **AMA** resulted a quite interesting inhibitor of NDM-1 (IC_{50} 7.0 μM) and of other MBLs as well, such as VIM-2 and IMP-7, whereas it resulted completely ineffective against SBLs.[81] The inhibition mediated by **AMA** is irreversible and the enzymatic activity can be restored only with a supplement of Zn(II) ion. NMR and mass spectrometry experiments revealed that **AMA** inhibits MBLs by sequestering the active site zinc ions, without removing them from the catalytic pocket.[82]

AMA resulted particularly effective in targeting the less tightly bound Zn2, whereas to sequester Zn1 higher **AMA** concentrations are required.[83] The co-administration of **AMA** and MEM showed a synergistic effect in NDM-1 expressing carbapenemase-resistant strains of Enterobacteriaceae.

Susceptibility was restored in over 80% of clinical isolates of *Acinetobacter* and *Pseudomonas*.[81] **AMA** possesses three stereogenic centers. Lederer, Moller and co-worker proposed that the absolute configuration of **AMA** was 2"R,2'R,2S or 2"S,2'S,2S .[79,84]

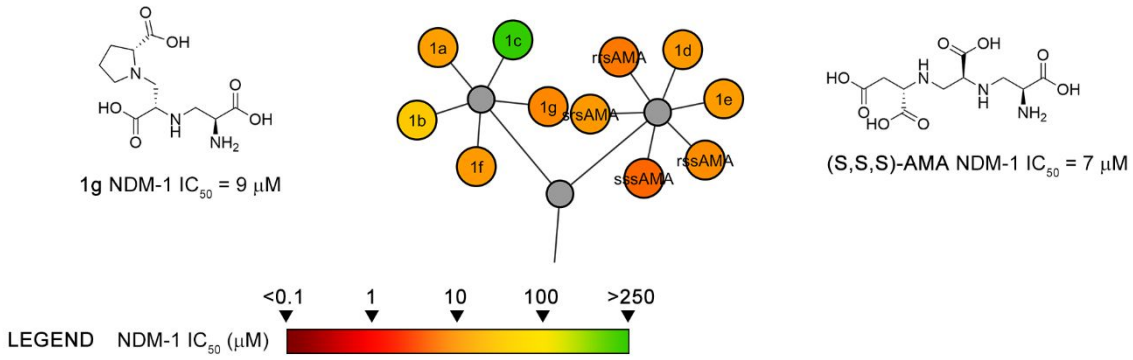

Figure 10. NDM-1 inhibitors structurally related to AMA.

However in 2016 Lei, Wright and co-workers carried out the first stereoselective synthesis of the molecule, reassigning the absolute configuration of the three stereocenters to (S,S,S). (**S,S,S)-AMA** showed the same inhibitory activity against NDM-1 as the first natural extract, whereas the first proposed (**R,R,S)-AMA** resulted completely inactive.[85,86] The development of a total and stereoselective strategy for the synthesis of **AMA** opened the way to the synthetic optimization of **AMA**. Zhang and co-workers prepared seven new analogues (**1a-g**), protected or modified at the carboxyl groups in position C1 and C4 or at the amino group at the C9 position (**Figure 11**). Configurational isomers of **AMA** showed a comparable activity with respect to the natural extract suggesting that the configuration of the three stereocenters has no impact on the activity. On the contrary, the presence of carboxyl groups in C1 and C4, as well as of the carboxyl groups in C6 and C9, resulted critical for the activity, whereas the replacement of the aspartate residue with a proline retained a comparable activity (**1g**, **Figure 10**).[87] Synergy studies of **AMA** derivatives in combination with MEM on *K. pneumoniae* expressing NDM-1 showed that **AMA** stereoisomers performed better than **AMA** analogous, but only **(S,S,S)-AMA** presented the best synergic effect.[87]

The capability of **AMA** to inhibit MBLs by sequestering the zinc ions suggested the use of chelating agents as a possible way to overcome MBL-mediated antibiotic resistance.[88] Somboro *et al*. explored the capability of 1,4,7-triazacyclononane-1,4,7-triacetic acid (**NOTA, Figure 12)** and 1,4,7,10-

tetraazacyclododecane-1,4,7,10-tetraacetic acid **(DOTA)** to restore the activity of carbapenems on NDM-1-producing bacteria. The MEM/**NOTA** combination restored the antibiotic susceptibility and resulted 32-times better than MEM/DOTA. Similar synergic effect was observed with IPM/**NOTA** as well.[89] Based on these promising results, Zhang *et al*. synthesized and evaluated a series of **NOTA** dithiocarbamate derivatives as MBLs inhibitors (**2a-h**). Only compound **2e** (sodium 1,4,7-triazonane-1,4,7-tris-carboxylodithioate, **Figure 12**) was able to restore the activity of MEM in clinical carbapenem-resistant Enterobacteriaceae (CRE) carrying *bla*NDM-1. The inhibitor activity depends on the capability of **2e** to chelate the zinc ion.

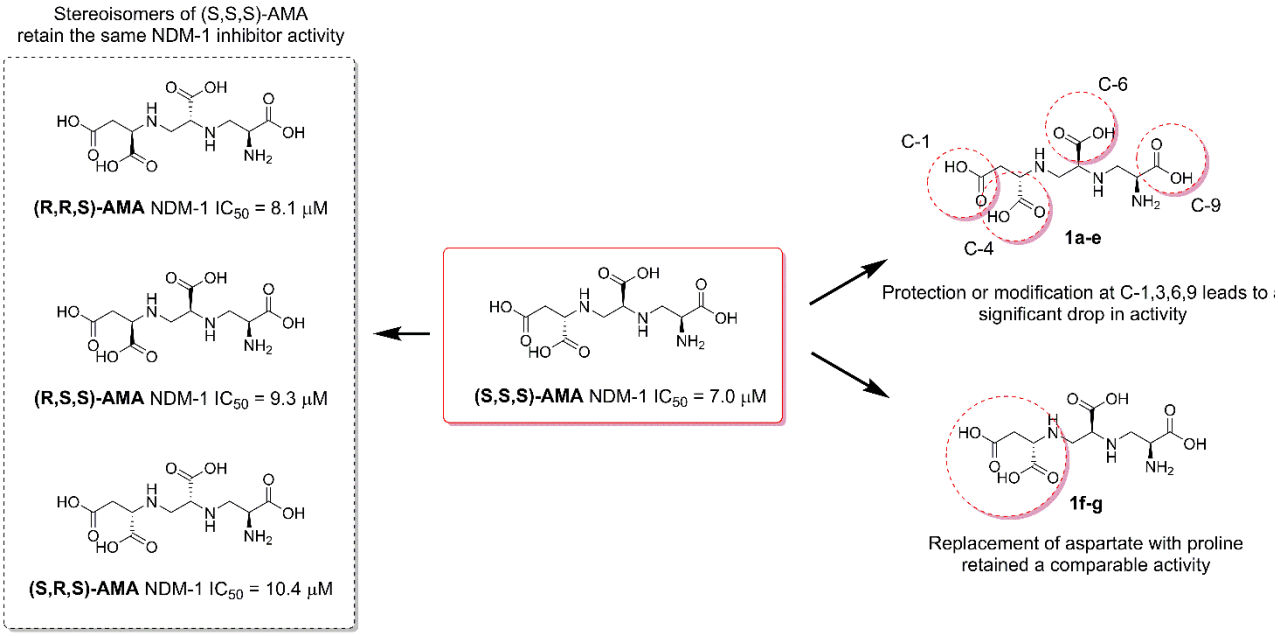

Figure 11. Chemical structures and Structure Activity Relationship (SAR) of **AMA** stereoisomers and derivatives.

The capability of a dicarboxylic acid metal chelator (disodium 2,3-diethylmaleate, **DEM**) to potentiate carbapenem activity against Enterobacteriaceae and *A. baumanii* expressing diverse MBLs, including NDM-1, was phenotypically studied by Livermore *et al*.[90] **DEM** synergized with carbapenems and cephalosporins against all the Enterobacteriaceae expressing MBLs. The synergistic effect was more effective on strains producing VIM than NDM-1. No effect was detected on SBLs expressing strains.

Lately, Schnaars *et al*. reported the synthesis and the biological evaluation of a series of tris-picolylamine (**TPA**) derivatives (**Figure 12**). **TPA**, a strong and selective zinc chelator, was linked

to small peptides in order to improve its physicochemical properties (**3e-o**). These peptides were able to restore MEM activity against clinical strains of *P. aeruginosa* and *K. pneumoniae* expressing VIM-2 and NDM-1, resulting in a MIC reduction of MEM of 32-256-fold at 50 μM. The best peptide, **3k** (**Figure 12**), showed low micromolar affinity for NDM-1 and resulted active against three additional clinical strains expressing MBLs (i.e. *K. pneumonia* VIM-1, *E.coli* NDM-1 and *E.coli* VIM-29) but not against strains expressing SBLs (i.e. GES-5, KPC-3 and OXA-48), supporting zinc chelation as mechanism of action.[91]

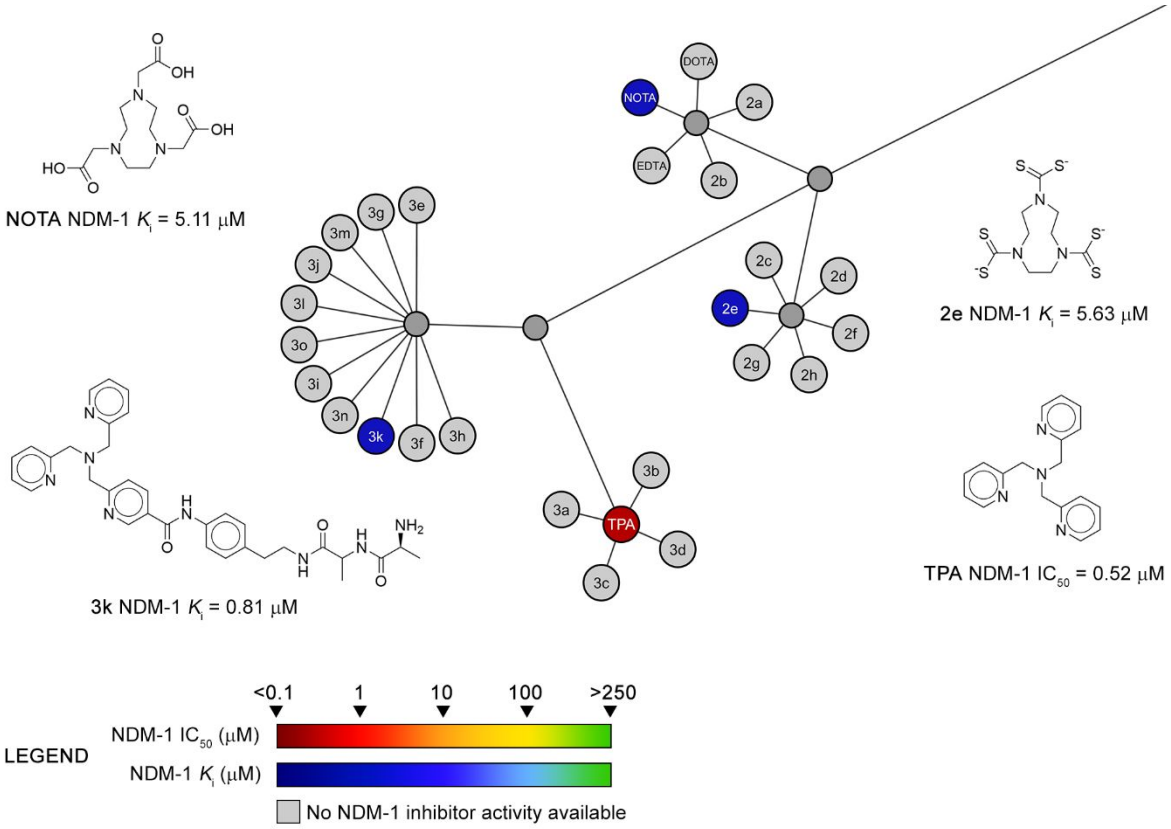

Figure 12. Chelating agent: **NOTA**, its derivative (**2e**), TPA and its peptide **3k**.

Molecules coordinating the zinc ions

Mercapto aliphatic acid

To design more selective and less cytotoxic MBLs inhibitors, molecules able to coordinate the zinc ions within NDM-1 binding site were designed (**Figure 13**).[14]

L-Captopril, a drug approved as ACE-inhibitor in the treatment of hypertension [92] is also known as active MBLs inhibitor.[93] Notably, the presence of thiol moieties among MBL inhibitors is quite

common.[94,95] Guo *et al*., observed that **D-captopril** (**Figure 13**) possesses a high inhibitory activity against NDM-1 with an IC_{50} of 7.9 μM, whereas the L enantiomer resulted 25-fold less potent.[96] The binding of the drug to NDM-1 was first analysed by mass spectroscopy and a year later by X-ray crystallography. King *et al*. solved the first crystal structure of **L-captopril** in complex with NDM-1.[21]

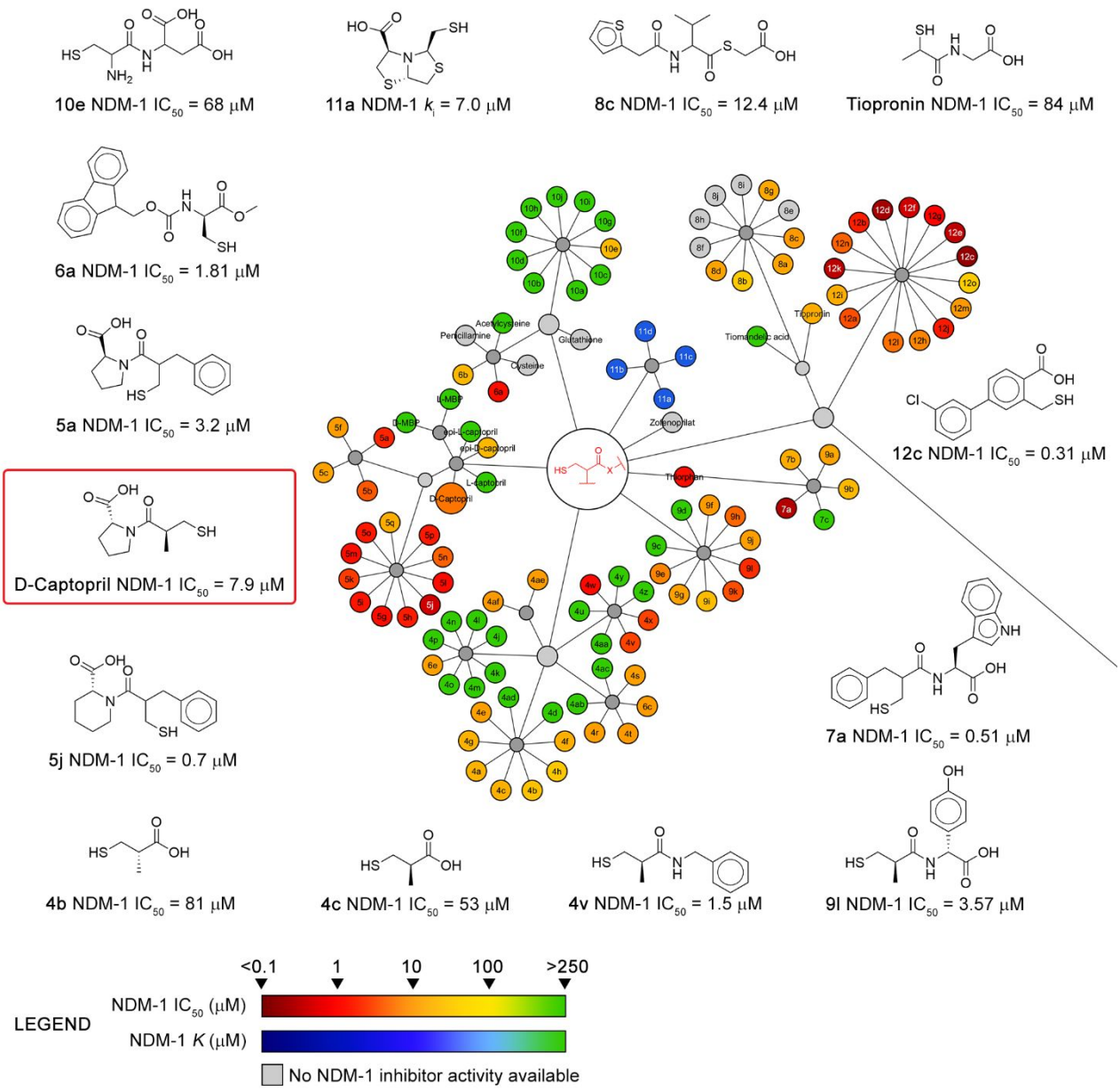

Figure 13. Mercapto aliphatic acid derivatives acting as zinc coordinating inhibitors.

In X-ray structure, the thiol moiety of **L-captopril** intercalates between the two Zn ions, displacing the water molecule and acting as a competitive inhibitor of NDM-1. In addition, the hydrophobic part of the molecule interacts with the L3 loop, whereas the hydrophilic part of the drug is involved in a hydrogen bond with Asn220, a residue involved in substrate binding and in intermediate product stabilization (**Figure 14**). To estimate the binding of the more active enantiomer **D-captopril** within NDM-1 active site, the crystal structure of BlaB:**D-captopril** was assumed as reference.[97] BlaB and NDM-1 share a high amino acid sequence identity within the binding site as per zinc ions coordination as per key amino acids involved in the catalytic activity. Therefore, it was hypothesized that **D-captopril** could adopt the same general binding orientation in NDM-1 as that determined for BlaB. Interestingly, superimposing BlaB:**D-captopril** and NDM-1:**L-captopril** X-ray structure, the two diastereomers appear to bind in a different orientation, but with the thiol-moiety still intercalating between the two zinc atoms and disrupting the nucleophile from its active orientation.[21,96]

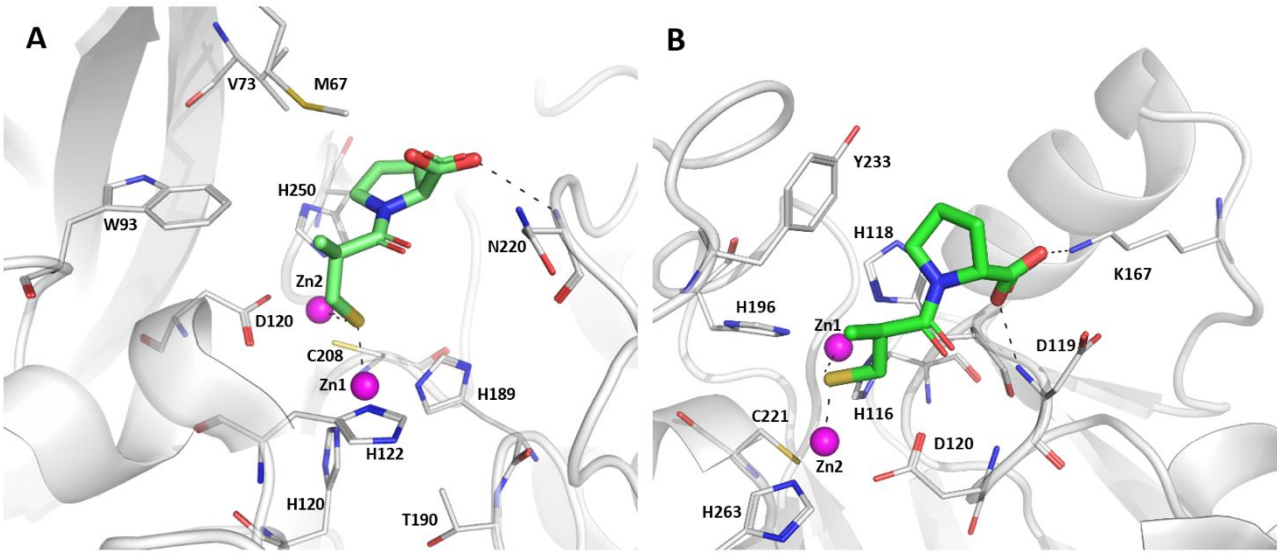

Figure 14. **L-Captopril** binding orientation in NDM-1 (**A**) and BlaB (**B**) catalytic site (PDB code 4exs and 1m2x, respectively).[21] The ligand is shown in green capped stick while the binding site residues in grey capped sticks. The zinc ions are displayed as magenta spheres. The hydrogen and coordination bonds are represented in black dashed lines.

A study performed by Brem J. *et al*. on the inhibition of NDM-1 and other MBLs (IMP-1, VIM-2 and SPM-1) by four captopril stereoisomers and the D- and L- enantiomers of captopril derivative 1-(2-mercaptobenzoyl)pyrrolidine-2-carboxylic acid (**D-** and **L-MBP**) confirmed the importance of the stereoisomerism for improving potency and selectivity against MBLs. **D-captopril** still remained the

most active NDM-1 stereoisomer. Structural analysis showed for **D-captopril** a binding mode similar to that of hydrolyzed β-lactams (PDB entry 4HL2),[98] especially penicillins.[99]

The ligand coordinates through the thiol moiety the two zinc ions. Thiols in MBL binding sites undergo a 100-fold pK_a decrease.[21,100] Therefore, at physiological pH the deprotonated thiolate will result a better metal coordinator. An additional hydrogen bond is formed between the ligand carboxylic group and the backbone nitrogen of Asn220. The carboxylic moiety, however, is quite solvent exposed and the aforementioned bond does not likely stabilize the ligand, as also supported by the alternative orientation assumed by Asn220 in chain B (PDB: 4exs) Hydrophobic interactions are additionally formed between the methyl and pyrrolidine moieties with residues Met67 and Trp93.

The identification of captopril as a potent NDM-1 inhibitor able to coordinate the catalytic site zinc ions represented the starting point for the development of new inhibitors bearing both thiol and carboxylic moieties capable of metal ligation. In a first attempt, Klinger *et al*. screened, against NDM-1, VIM-2 and IMP-7, a set of eleven approved drugs possessing a sulfhydryl moiety.[101] Interestingly, not all the selected drugs, **thiomandelic acid**, **DL-captopril**, **DL-thiorphan**, **N-acetylcysteine**, **meso-2,3-dimercaptosuccinnic acid**, **2,3-dimercaprol**, **D-penicillamine**, **glutathione**, **L-cysteine**, **zofenoprilat** and **tiopronin** (**Figure 13**) inhibited the three considered MBLs with the same potency. **D-captopril** showed a low micromolar inhibitory activity against NDM-1 in line with the affinity detected *vs* VIM-2 and IMP-7. Focusing on NDM-1, **thiorphan** and **dimercaprol** resulted the most active drugs but still in the low micromolar range. On the contrary, **tiopronin** showed only a modest activity, whereas **N-acetylcysteine** resulted completely inactive. Thermal shift assay confirmed the ligands capability of binding without sequestering the zinc ions. The binding mode of **tiopronin** was confirmed by X-ray crystallography (PDB: 5A5Z).[102] In the complex, the ligand thiol moiety of **tiopronin** intercalates between the two zinc atoms, thus replacing the catalytic water in a similar way to that observed for captopril. Compounds showing more potent inhibition and positive response in thermal shift assay were further tested for synergy in combination with IPM against *E. coli, P.aeruginosa* and *K. pneumoniae* strains over-expressing NDM-1, IMP-7 and VIM-1. **Thiorphan** and **dimercaprol** were able to potentiate IPM activity reducing the MIC values from 2 to up 64-fold.[101]

Later, Li *et al*., in an effort to simplify captopril structure and identify the chemical features critical for molecular recognition in NDM-1, synthesized and tested a series of 3-mercapto-2-methylpropanoyl amides (**4a-f, Figure 13**). The 3-mercapto-2-methylpropanoic acid enantiomers and their methyl ester derivatives, revealing that the thiol group and the free carboxylic moiety are essential for binding. The two enantiomers (**4b** and **4c, Figure 13)**, in fact, displayed a similar affinity, whereas the esterification led to a complete loss of activity. Retaining the 3-mercapto-2-

methylpropanoyl moiety of captopril, the proline residue was further replaced by aliphatic and aromatic amines (**4d-4ad**). Derivative **4v** (**Figure 13**) resulted the most potent NDM-1 inhibitor in this series.[103]

Recently, Buttner *et al*. reported the investigation of a series of thiol-derivatives inspired by captopril (**5a-q, Figure 13**). Structural modifications on the pyrrolidine ring (e.g. ring simplification, contraction or expansion, ring bioisosterism and variation of the position of the acidic group) and on the methyl group (e.g. introduction of an aromatic ring) were tested. SAR studies against NDM-1 revealed that the introduction of an unsubstituted phenyl ring (**5a, Figure 13**) maintained an activity comparable to that of captopril, whereas the introduction of substituents on the thiophene ring led to a potency decrease. All the modifications introduced on the proline-moiety of captopril led to the more active derivatives **5g-o**. Interestingly, compound **5j** (**Figure 13**) resulted 7-fold more potent than its enantiomer **5k**, confirming the importance of stereoisomerism in the development of NDM-1 inhibitors. Docking calculations supported this evidence, predicting a key interaction between **5j** and Lys211, a residue normally involved in substrate orientation and hydrolysis. Between the two piperazine derivatives (**5p-q**) only **5p,** carrying a benzoyl group in position 4, resulted as potent as captopril and **5j-k**. Compound **5a** and **5j** were evaluated *in vitro* in combination with IPM against resistant clinical isolates. Both **5a** and **5j** showed a 16-fold MIC reduction against *E. coli* pET24a T2377, but resulted ineffective against *K. pneumonia* T2301. However, captopril, assumed as the reference compound, still performed best in restoring IPM activity.[104]

Other NDM-1 inhibitors, structurally related to captopril and carrying a 3-mercapto-propionic acid moiety or a cysteine-based scaffold, were identified through ultrafiltration C/MS-based assay by Chen *et al*. (**6a-e, Figure 13**), with **6a** showing low micromolar affinity for NDM-1.[105]

Similarly, combining both phenotypic and target-based screening by NMR spectroscopy on a library of 92 known MBLs inhibitors, Ma *et al*. were able to identify compound **7a** (**Figure 13**) as a low micromolar NDM-1 inhibitor.[106]

In an effort to discover new MBLs, Liu *et al*. synthesized and evaluated ten mercaptoacetic acid thioester amino acid derivatives (**8a-j, Figure 13**), which showed a micromolar-nanomolar inhibition of L1, a di-nuclear MBL belonging to subclass B3. Some of the thioesters resulted effective toward NDM-1 and their binding mode investigated *in silico*.[107]

The authors recently published a new set of 2-substitued (S)-3-mercapto-2-methylpropanamido-acetic acid derivatives (**9a-l**),[108] modifying a library of 3-oxoisoindoline-4-carboxylate derivatives active against VIM-2.[109] The compounds resulted to be potent nanomolar inhibitors of VIM-2 and low micromolar inhibitors of NMD-1, with **9k** and **9l** being the most active in the series (**Figure 13**). Kinetic enzymatic study on VIM-2 at different Zn ions concentration showed that the compounds

were not strong Zn chelators, similarly to captopril. Unfortunately, no structural data against NDM-1 enzyme are actually available. However, the superimposition of the available crystallographic structure of VIM-2:**9l** (PDB: 5Y6E) with the X-ray structures of NDM-1 complexed with hydrolyzed benzyl-penicillin and hydrolyzed cephalosporin suggested that these inhibitors bind the zinc ions and the catalytically important residues. The carboxylate group of **9l** interacts in VIM-2 with Arg205, like in NDM-1 the cephalosporin C4 carboxylic group interacts with Lys211, suggesting that inhibitors able to mime the hydrolyzed substrate could result valuable MBL inhibitors.[108] Importantly, the compounds showed no toxicity against HEK293T cells nor teratogenicity on embryo zebra fish.

Starting from the validated 3-mercapto-proprionic acid moiety, Shen *et al*. recently disclosed the results obtained with a series of ten oligopeptides (**10a-j**), carrying a cysteine residue as the key chemical feature. The dipeptide **10e** (Cys-Asp, **Figure 13**) presented the highest potency. None of the compounds showed antibacterial activity *per se*, but **10a, 10b, 10e** and **10g** in combination with ertapenem showed synergic activity against *E. coli* and *P.aeruginosa* strains overexpressing NDM-1. In particular, **10e** reduced the MIC of ertapenem to < 128 μM against *E. coli* and *P.aeruginosa* strains, at a concentration of 25 μM. The binding mode of **10e** within the NDM-1 active site was investigated by docking calculations, suggesting the formation of key interactions between the thiol and Zn1 and His120, and between the aspartate and Zn2.[110]

A new chemical scaffold (bisthiazolidine, BZTs) was designed by Gonzales *et al*., combining the mercapto-propionic acid moiety with features of β-lactam substrates (**11a-d, Figure 13**). BTZs bicyclic system could mime a non-cleavable β-lactam ring. While the bridging nitrogen and the carboxylate interacting with Zn2 are retained, other zinc-binding groups are additionally inserted in the structure. The four bisthiazolidines disclosed by the authors resulted to act as low micromolar competitive inhibitors. *In vitro* NMR studies on NDM-1 producing *E. coli* strains, demonstrated that the compounds are able to inhibit the hydrolysis of IPM by NDM-1 with micromolar affinity. The crystal structure of the NDM-1:**11a** complex (PDB 4u4l)[111] was also resolved. **11a** orients the thiol group between the two Zn ions and displaces the bridging water molecule. The carboxylic group does not directly bind the Zn ions, but interacts with Lys211 by means of a water molecule.[112] The four BZTs **11a-d** were able to reduce up to ten thousand folds the count of viable cells with respect to the antibiotic alone, when assessed against NDM-1-producing clinical isolates of *K. pneumoniae*, *A. baumannii*, and *P. rettgeri* in combination with IPM. BTZs also demonstrated to have a broad-spectrum of action against other MBLs subclasses and the ability to preserve β-lactam activity against important pathogens.[113]

Recently, Cain *et al.* reported the successful application of an *in silico* fragment-based design for the development of B1 MBLs (NDM-1, VIM-2 and IMP-1) inhibitors. Combining fragments in the

binding site, the benzyl thiol derivative **12c** (**Figure 13**) was identified as a possible NDM-1 competitive inhibitor. Docking calculations predicted that **12c** H-bonds through the carboxylate group to Lys224 and Zn2, the thiol group coordinates Zn1 and Zn2, while the aryl ring is involved in π-π stacking interaction with Trp93. When tested, compound **12c** showed a low micromolar affinity for NDM-1 and a submicromolar potency against VIM-2 and IMP-1. The replacement of the distal aromatic ring with substituents or heterocycles did not affect the potency of the designed inhibitors with respect to the starting lead. Compounds **12c** and **12i-o** were assayed in biological tests in combination with MEM against *E. coli* and *K. pneumonia* NDM-1 producing strains. The compounds reduced the MIC of MEM alone by 2-16-fold, with compound **12n** being the best candidate.[114]

Since mercapto-carboxylic acids demonstrated to be valuable MBLs inhibitor scaffolds, Skagseth *et al.* explored the importance of the carboxylic group by bioisosteric replacement (**Figure 15**). Starting from compound **13a** (**Figure 15**), the carboxylic group was replaced by phosphonate esters, phosphonic acid and tetrazoles. The effect of the chain length and of the mercapto functionality were also explored (**13a-p**) against VIM-2 and NDM-1. With respect to NDM-1, almost all the compounds resulted more active than the reference one **13a**.

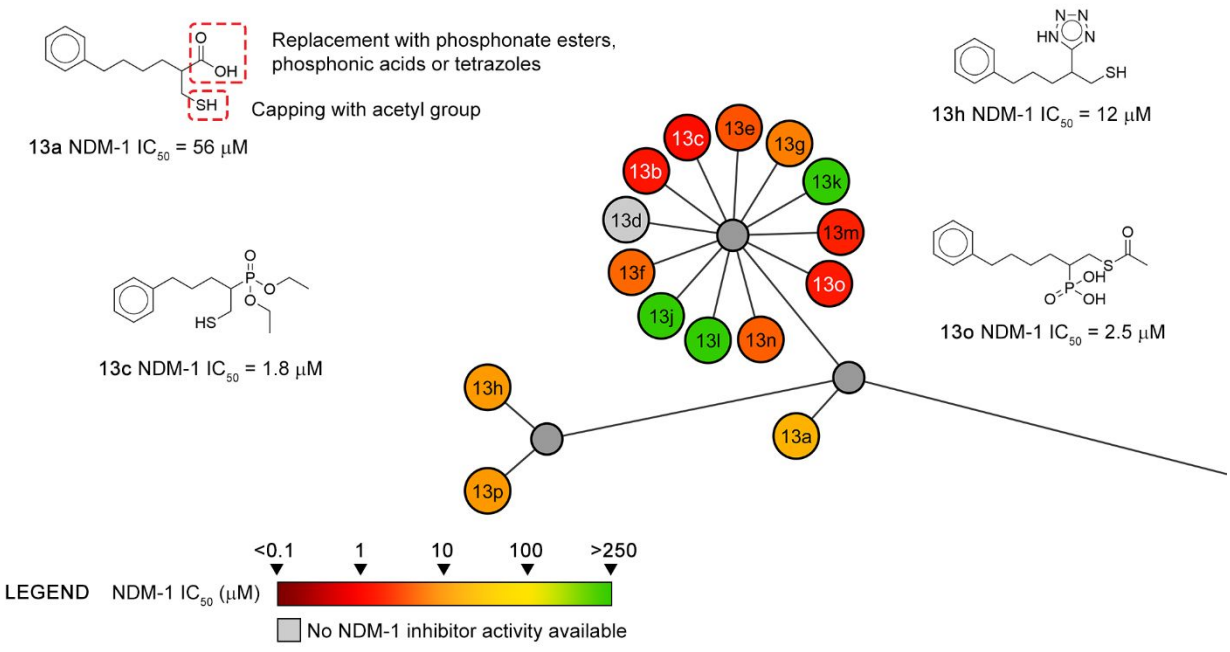

Figure 15. Mercapto aliphatic acid derivatives as NDM-1 inhibitors: exploring carboxylate bioisosters.

The most active compounds always presented a thiol (free or acetylated) and a phosphonic acid or ester in their structure. Tetrazole derivatives (**13h**, **Figure 15**) generally resulted less effective than

phosphonate compounds. Analogues **13c**, **13o** and **13p** were successfully crystallized only with VIM-2. Therefore, to assess the binding mode of these inhibitors within NDM-1 active site, docking calculations were performed and the binding mode compared to the X-ray pose observed in VIM-2. The inhibitors were predicted to bind the two catalytic zinc ions through the thiol functionality and Asn233 residue through the phosphonate group, as for VIM-2. However, the phenyl ring of the inhibitors resulted less stabilized by hydrophobic interactions in NDM-1 with respect to VIM-2, somehow explaining the corresponding slightly lower activity. All the inhibitors were tested for synergic activity with MEM against MBL-producing clinical strains of *P. aeruginosa* and *K. pneumoniae* showing only modest biological activity.[115]

Isatin-β-thiosemicarbazones and spiro[indole]thiadiazoles

Recently, following a drug repurposing approach, Song *et al.* identified **methisazone** (**Figure 16**) as a weak NDM-1 inhibitor.[116] **Methisazone**, an old drug used for the treatment of smallpox infections,[117] is structurally related to isatin, an endogenous natural product with a wide range of biological activities. Moving from this, Song *et al.* synthesized and tested *in vitro* several isatin-β-thiosemicarbazone derivatives, all sharing the methisazone scaffold. All the thirteen compounds (**14a-n**) showed a low micromolar NDM-1 inhibitor activity, with **14n** (**Figure 16**) being the most active one. Docking calculations predicted the sulphur atom to be oriented at coordinating distances from zinc ions.[116]

Falconer *et al*. reported a series of zinc-selective 3'H-spiro[indoline-3,2'-[1,3,4]thiadiazol]-2-one derivatives (structurally related to isatin-3-thiosemicarbazones) able to potentiate the antibacterial activity of β-lactams in *E. coli* strains overexpressing various MBLs (**15a-m**). One of the disclosed analogues, compound **15a,** was already reported to perturb iron homeostasis in bacterial cells.[118] The researchers, interested in exploring the zinc versus iron specificity, introduced a range of chemical modifications on **15a** main core. Selective modifications at the R1 position resulted in a zinc-specific profile. The most selective compound **15i** (**Figure 16**), in combination with MEM against clinical isolate of *K. pneumonia* harbouring *bla*NDM-1, restored susceptibility to the carbapenem. Moreover, compound **15i** resulted able to potentiate the activity of other carbapenems as well e.g. IPM, doripenem, and biapenem, whereas synergism was not observed in combination with non-carbapenem β-lactams.[119]

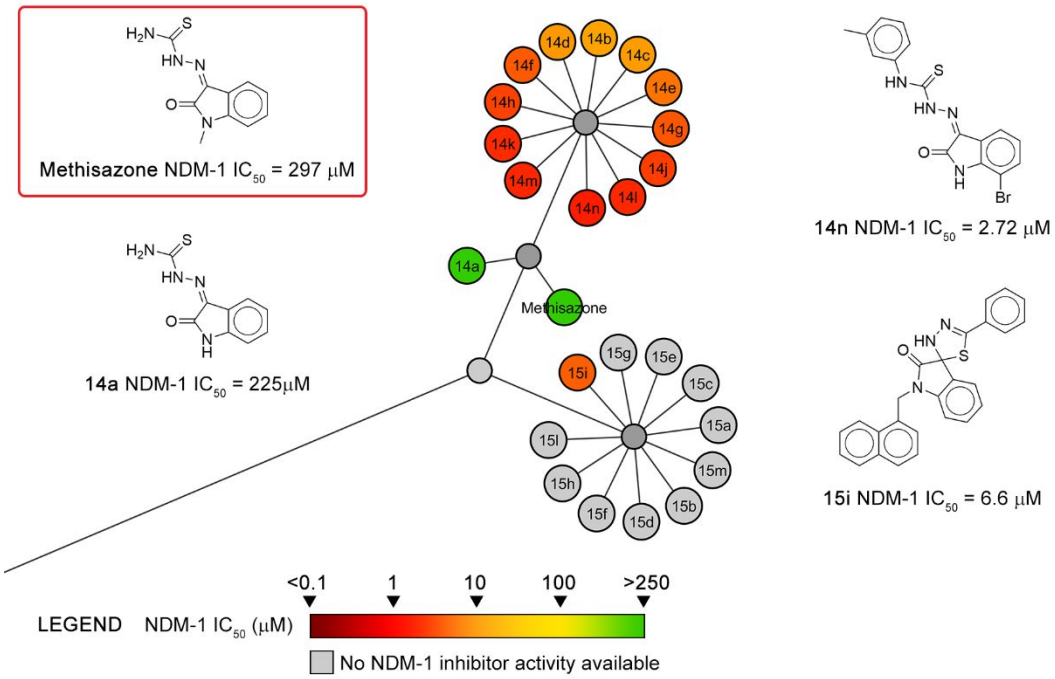

Figure 16. Methisazone optimization: exploring isatin-3-thiosemicarbazone and 3'H-spiro[indoline-3,2'-[1,3,4]thiadiazol]-2-one as valuable chemical scaffolds.

Azolylthioacetamide

Starting from a previous work on azolylthioacetamide as MBLs inhibitors,[120,121] Zhang *et al*. reported the synthesis and evaluation of new diaryl-substituted azolylthioacetamides (**16a-r, Figure 17**) as sub-micromolar inhibitors of NDM-1. Thirteen derivatives resulted to behave as mixed, low micromolar inhibitors toward NDM-1 and four of them showed broad-spectrum activity against other MBLs such as CcrA, ImiS and L1. Docking predictions for **16d** and **16i** (**Figure 17**) suggested that the deprotonated triazoles coordinate the two zinc ions, whereas the N-phenylthioacetamide moiety binds to an alternative binding site. In particular, the 2-phenolyl hydroxyl group of **16i** resembles the hydrolyzed benzyl-penicillin as observed in the crystal structure of NDM-1, thus mimicking the C3 carboxylate and interacting with Lys211.[122] Based on these results, Zhai *et al*. replaced the azolylthioacetamide scaffold with triazolylthiacetamide in a library of twenty-four new derivatives (**17a-x, Figure 17**), which all showed sub-micromolar IC_{50}. Kinetic characterization of compounds **17v** and **17r** (**Figure 17**) revealed a partially mixed mechanism of inhibition with K_i of 0.49 and 0.63 μM, respectively.[123] Docking calculations on these two inhibitors suggested binding orientations similar to the azolylthioacetamides analogues.[122-123] To enrich the structure-activity relationship among azolylthioacetamide derivatives (**18a-ab, Figure 17**), the authors explored four homologous

of the azolyl ring (triazole, oxadizole, thiadiazole, and 1-amino-triazole) and structural modifications on the aromatic portion of the central scaffold.[124] Compounds **18a-s**, possessing unsubstituted benzimidazole or benzoxazole rings, resulted to selectively inhibit B2 ImiS (IC_{50} in the low-sub micromolar range), without showing any significant activity against NDM-1. On the contrary, the introduction of a nitro group in position 5 on the benzimidazole scaffold (**18t-ab, Figure 17**) improved the activity toward NDM-1, suggesting that the nitro group could be involved in binding the Zn ions. Docking calculations on compound **18aa** (**Figure 17**), in fact, suggested a completely different binding mode with respect to that observed for ImiS analogue inhibitors. The triazole ring of **18aa** does not interact with the two Zn ions, whereas the nitro group is able to intercalate Zn1 and Zn2 in NDM-1 active site. Kinetic studies performed on the best inhibitor revealed a competitive and uncompetitive mixed inhibition kinetic pattern that need further investigation. Finally, synergy studies, conducted in combination with IPM against clinical strains of *E. coli* expressing ImiS and NDM-1, showed a 2-4 folds MIC reduction consistent with the *in vitro* activity.

The effectiveness of the 2-mercapto-triazole scaffold was further validated by a recent structure-based virtual screening performed by Spyrakis *et al*. on a large database of available chemicals.[125] All the 31 potential active candidates were characterized by the presence of electron-donor groups able to coordinate the zinc ions. The best inhibitors **19a** and **19b** (**Figure 17**), sharing a 2-mercapto-triazole moiety showed a K_i against NDM-1 of 0.72 and 1 μM, respectively. Based on the docking prediction, compounds **19a** and **19b** interact with the zinc ions via the thiol and the nitrogen of the triazole ring, whereas the substituent in position 5 on the heterocyclic ring points toward the hydrophobic hot spots of the catalytic pocket (loop 3). Further interactions involved nitrogen-1 of the ring with Lys211. Moreover, compound **19b** contacts both zinc ions with the thiol moiety and forms additional interaction with Asn220. Both compounds **19a** and **19b** were tested in combination with MEM via microdilution drug−drug interaction assays against *E. coli* clinical isolate carrying *bla*NDM-1, and against *E. coli* BL21 (DE3) recombinant strain overproducing NDM-1. Both of them reduced the MIC of MEM in the clinical isolate and in the recombinant strain up to 16-fold. Inhibitors possess a full synergic profile as *per* FICI (Fractional Inhibitory Concentration Index) results.[125] The work performed by Spyrakis *et al.* represents, among others here cited, a successful story of *in silico* studies applied to NDM-1 inhibition.[67,125–127] The application of high-throughput docking methods along with the availability of large chemicals databases can represent a powerful tool in the identification of new NDM-1 inhibitors, allowing the identification of new compounds to inhibit clinically-relevant MBLs.

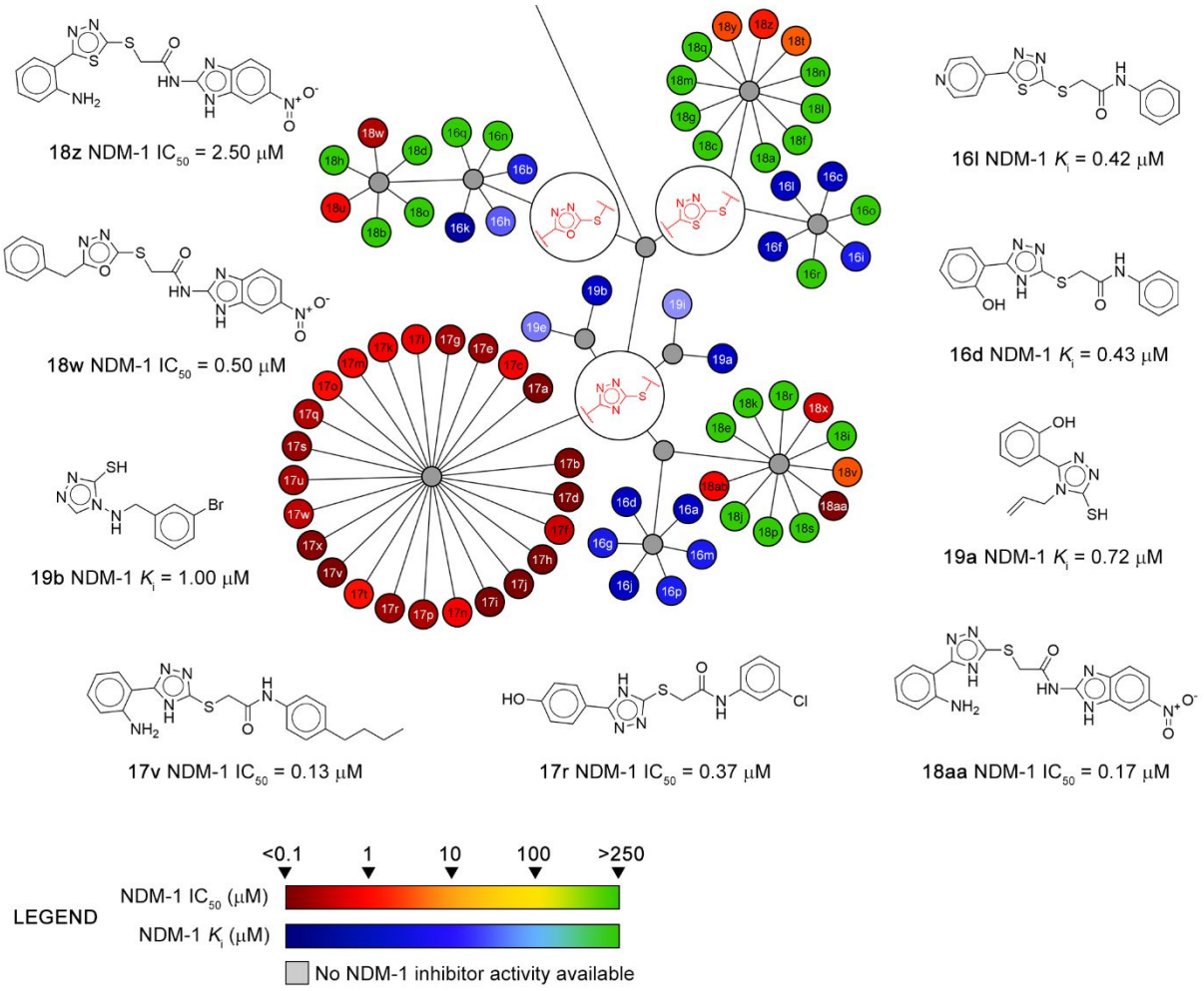

Figure 17. 2-mercapto-azoles derivatives as NDM-1 inhibitors.

Rhodanine

Rhodanines have been reported as effective non transitional state analogues of SBLs[128] and Penicillin Binding Proteins (PBPs).[129] Recently, Spicer *et al.* observed the capability of this chemical scaffold to inhibit also B1 MBLs, as VIM-2 and IMP-1.[130] In an effort to develop broad-spectrum MBL inhibitors, Xiang *et al*. designed and synthesized twenty-six rhodanine derivatives (**20a-aa, Figure 18**), exploring diverse aromatic rings and substituents on the core ring.[131] The compounds were assessed for their enzymatic activity against B1 MBLs (NDM-1 and VIM-2), B2 MBL (ImiS) and B3 MBL (L1). In particular, for NDM-1, compounds **20b, 20g, 20i–l, 20n-q**, and **20t-z** showed an interesting potency, with **20o (Figure 18)** being the most active. All the compounds showed submicromolar/nanomolar activity against L1 and VIM-2 and low micromolar activity against ImiS. In particular, **20y** (**Figure 18**) resulted the most potent broad-spectrum inhibitor in the series. The binding mode of **20y** in NDM-1 predicted by docking simulation is shown in **Figure 19**. The nitro

group contacts a zinc ion and Asp124, while the benzene ring at the R1 position forms π–π stacking interaction with Phe70. Further studies performed by Brem *et al.* suggested that thienolate, the hydrolysis product of rhodanine, has activity against MBLs as well.[132]

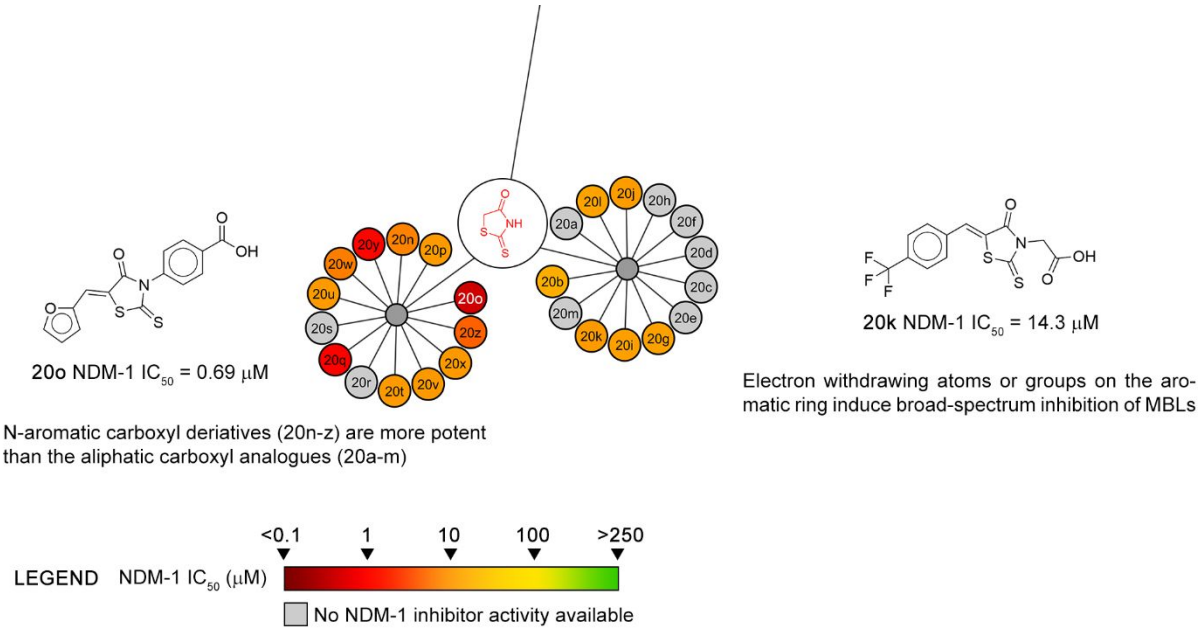

Figure 18. Rhodanine derivatives: chemical structure and inhibitor activity against NDM-1.

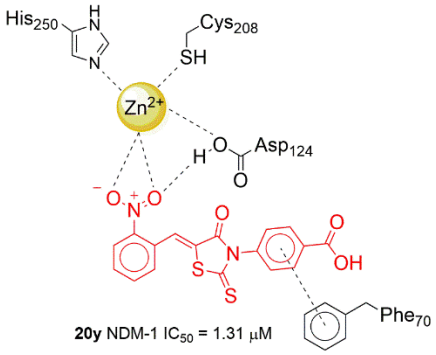

Figure 19. Derivative **20y** predicted binding mode and enzymatic inhibitor activity *vs* NDM-1.

Following this finding, the authors prepared thienolate analogues (**20aa**) of **20t**, finding that the compounds were able to inhibit only VIM-2 and L1, but not NDM-1 and ImiS. The structure–activity relationship revealed that N-aromatic carboxyl (**20n-z**) derivatives are more potent than the aliphatic carboxyl analogues (**20a-m**), implying that the phenyl ring may interact with the hydrophobic pocket of MBLs. In addition, diaryl-substituted rhodanines with electron-accepting atoms or groups (**20t–z**)

exhibit broad-spectrum inhibition of MBLs. The co-administration of the compounds at a concentration of 32 μg/mL with cefazolin resulted in a 4-8 fold MIC reduction in *E.coli* strains expressing NDM-1.[131]

Dipicolinic acid

Chen *et al*. recently reported the results obtained with a fragment-based drug discovery approach, by which 2,6-dipicolinic acid was identified (**DPA**, **Figure 20**) as a valuable chemical scaffold for the development of new NDM-1, and related MBLs (IMP-1 and VIM-2), inhibitors.[133] **DPA** showed an IC_{50} of 520 nM toward NDM-1 and was chosen for further chemical elaborations. Forty-seven **DPA** derivatives (**21a-aq, Figure 20**) were synthesized and divided into three subseries. The first series consisted of compounds obtained by substituting one of the carboxylic moieties of **DPA** with various amide (**21a-r, Figure 20**). The second series consisted of **DPA** derivatives substituted in position 4 with aliphatic and aromatic rings connected with an amine linker (**21s-ab, Figure 20**). Finally, the third series consisted of biphenyl-DPA derivatives (**21ac-aq, Figure 20**). The first series (**21a-r)** resulted poorly active against NDM-1, with the only exception of compounds **21i** and **21l**. The second series (**21s-ab)** resulted more potent, with IC_{50} in the low micromolar range. More interestingly, the third series (**21ac-aq)** showed sub-micromolar IC_{50}. Among all the prepared derivatives, **21af** was the best identified inhibitor with nanomolar affinity. Further investigations revealed that, whereas **DPA** displayed a propensity to chelate metal ion from NDM-1, **DPA**-derivatives (such as **21aq**) can form a stable NDM-1:Zn(II):inhibitor ternary complex. MIC assays revealed the ability of **21aq** to reduce IPM MICs up to 32-fold vs *E. coli* and up to 16-fold vs *K. pneumoniae* strains carrying *bla*NDM-1.[133]

Starting from the **DPA** scaffold, Hinchliffe *et al*. recently reported the discovery of 6-phosphonomethylpyridine-2-carboxylates as MBLs inhibitors (**22c-f, Figure 20**).[134] Compounds containing a phosphonate moiety are known to chelate zinc ions and to inhibit metalloenzymes.[135] In addition, some phosphonates have been already reported as SBLs inhibitors, resembling the tetrahedral intermediate of the hydrolytic path.[136-115] The authors replaced one of the **DPA** carboxylic groups with a phosphonate, resulting in compounds **22c-e**. In compounds **22a** and **22b** one of the carboxylic group of **DPA** was removed without introducing the phosphonate, to evaluate the effect of the two carboxylic moieties in **DPA**. In **22f** both carboxylic groups were removed, introducing the phosphonate, to estimate the prevalence of the two groups. All the six compounds were assayed for their inhibitor activity against four MBLs (VIM-2, NDM-1, IMP-1 and L1). Focusing on NDM-1, compounds **22a-b** resulted inactive, highlighting the importance of having two carboxylic moieties. On the contrary, phosphonates **22c-e** showed interesting submicromolar activity. The presence of

both carboxylic and phosphonic acids seemed to be an important feature to achieve inhibition, whereas the presence of phosphonic acid alone (**22f**) was not enough to maintain potency (IC_{50} > 1000 μM). The superposition of the IMP-1:**22c** complex with NDM-1:hydrolyzed cephalexin showed how **22c (Figure 20)** replicates some aspects of interactions of MBLs with their β-lactam substrates. Compound **22c** was assessed for *in vitro* studies in combination with MEM against clinical isolates overexpressing MBL. At a concentration of 64 mg/L, **22c** was able to reduce the MIC of MEM up to 256 folds against *K. pneumoniae* expressing NDM-1.[134]

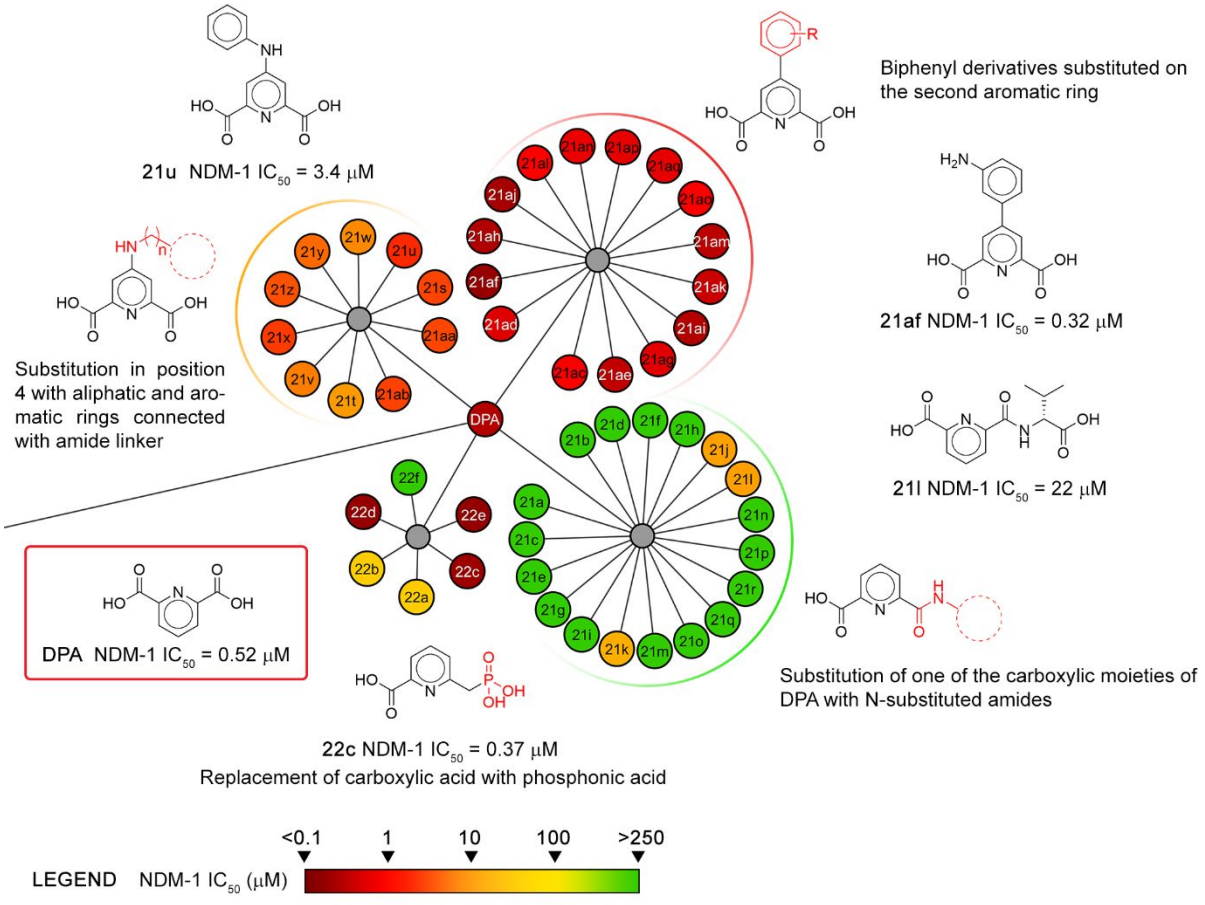

Figure 20. Detail of NDM-1 inhibitors dendrogram, focusing on dipicolinic acid (DPA) derivatives.

Cyclic and acyclic boronic acids

Inhibitors able to mimic the substrate transition state are well described in the literature for both SBLs and PBPs.[51] Tetrahedral intermediates as boronic acid derivatives mimic the transient oxyanionic specie produced by the nucleophilic attack of the catalytic serine on the β-lactam carbonyl. The

hydrolysis catalysed by MBLs evolves through the formation of a tetrahedral intermediate as well, therefore this inhibition strategy could be exploited also to target MBLs. Vaborbactam (VAB; formerly RPX7009) is a cyclic boronic acid with potent inhibitory activity against class A and C BLs. It is used in therapy in combination with MEM to restore the antibiotic activity against *K. pneumoniae* carbapenemase (KPC-2). However, **VAB** does not inhibit class B nor class D carbapenemases .[137,138] To identify more potent broad-spectrum inhibitors Brem J. *et al*. investigated the activity of other cyclic boronic acid derivatives (**23a-e, Figure 21**) against a panel of SBLs and MBLs (including NDM-1). All five compounds showed submicro/nanomolar inhibitor activity against NDM-1 and other MBLs and SBLs, acting as the first reported dual inhibitors. In particular, derivatives **23c** and **23e,** bearing an aromatic side chain in a position corresponding to β-lactam R_1 side-chain, resulted potent NDM-1 inhibitors (**Figure 21**).

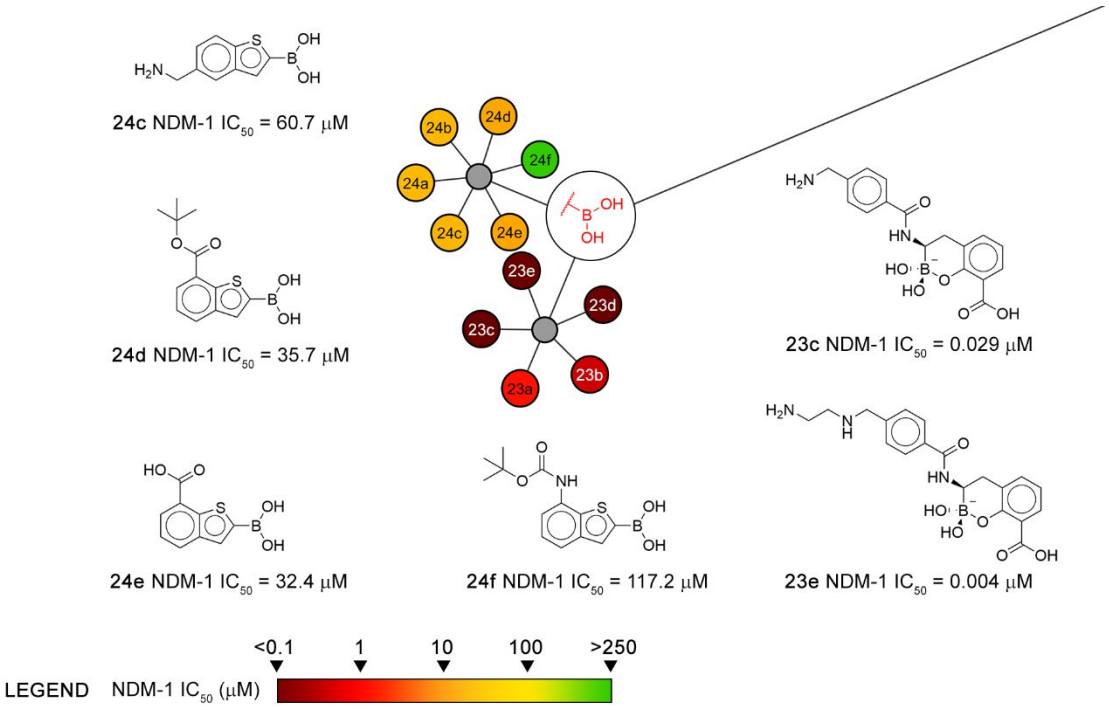

Figure 21. Cyclic and acyclic boronic acids as dual BLs inhibitors

The X-ray crystallographic structures of BcII and VIM-2 in complex with **23c** revealed binding modes similar to those observed in B1 MBLs-hydrolyzed β-lactams complexes: (i) the C-3 carboxylate coordinates both Zn2 and Lys211 (NDM-1 and BcII) or Arg205 (VIM-2); (ii) the bicyclic

phenyl-boronate ring of **23c** is positioned similarly to the cephalosporin dihydrothiazine ring establishing hydrophobic interactions with the conserved Trp87 and Phe61 residues; (iii) the side chain of **23c** assumes the same orientation and binding mode of the side chain of cephalosporins; (iv) the C-6 carboxylate of the hydrolyzed β-lactam coordinates Zn1 and H-bonds with Asn220 side chain; (v) the two 'exocyclic' boron-bound hydroxyl mime the binding modes of the oxyanion intermediate (**Figure 22A**). Compound **23c** was tested in biological assays in combination with MEM against recombinant *K. pneumonia* and clinical strains of *K. pneumonia* and *E. coli*. These strains all carry NDM-1, together with multiple SBLs of different classes. **23c** was able to reduce the MIC of MEM in all the NDM-1 expressing strains, in the best case up to 64 folds.[139]

Interestingly, boronic acids have been used for many years for rapid BLs detection in phenotypic screening, chromogenic tests and double-disk diffusion tests. To this extend, Santucci *et al*. recently reported the development and characterization of a small library of acyclic boronic acids (**24a-f, Figure 21**) targeting both SBLs and MBLs, NDM-1 included.[140,141] The described compounds showed a low micromolar inhibitor activity against SBLs (i.e. AmpC, CTX-M-15 and KPC-2), while compounds **24d** and **24e** showed activity also toward MBLs, thus representing the first case of acyclic boronic acids with an extended spectrum profile (Class A-D). From docking calculations, **24a-f** were predicted to coordinate the two zinc atoms by means of the boronic group and to interact with key catalytic residues (**Figure 22B**). The co-administration of **24f** with ceftazidime to clinically isolated *E. coli* strains overexpressing NDM-1 revealed a reduction of the ceftazidime MIC up to 32 folds.[142]

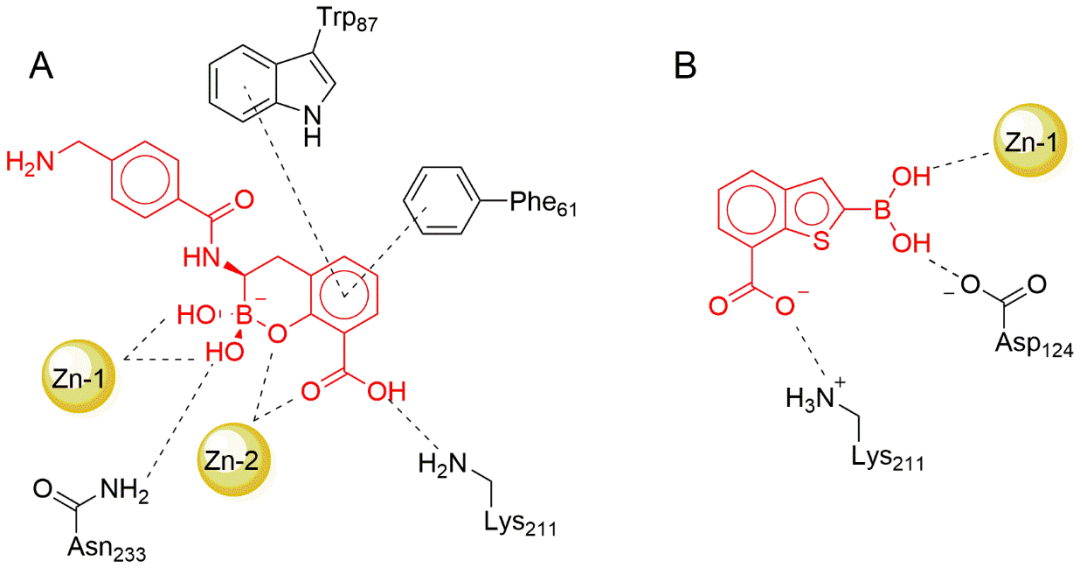

Figure 22. A) Compound **23c** binding mode within BcII active site; [139] B) Compound **24e** predicted binding mode within NDM-1 active site. [142]

1.1. Covalent inhibitors

Several β-lactams have been reported to perform a covalent and irreversible inhibition toward MBLs.[129,143] Thomas *et al*. observed how **cefaclor** (**Figure 23**) is able to inhibit in a time-dependent and irreversible manner NDM-1, with millimolar affinity. Unfortunately, supratherapeutical doses (>60 folds than the therapeutic plasma concentration) are needed to effectively inhibit NDM-1, thus preventing the use of this drug for the treatment of NDM-1-mediated bacterial infections. In particular, kinetic analysis, site-directed mutagenesis and mass spectrometer assays revealed that at lower concentration, **cefaclor** behaves as a typical substrate and is released after hydrolysis, whereas at higher concentration it accesses an alternative binding mode, involving Lys211, leading to irreversible inactivation.[144]

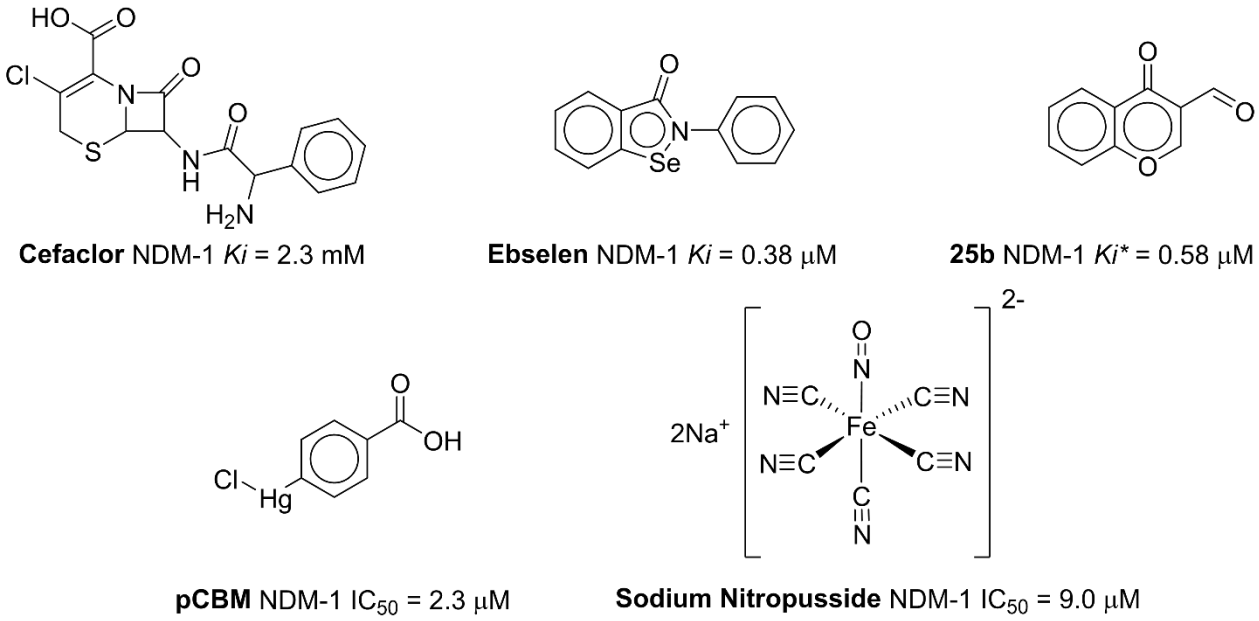

Figure 23. Covalent NDM-1 inhibitors: chemical structures and affinities.

In 2015, Chen *et al*., through a cell-based screening, reported the discovery of **ebselen (Figure 23)** as a new promising NDM-1 inhibitor. **Ebselen** is a drug currently in human clinical trials for the treatment of cerebral ischemia and stroke, with low toxicity in animal model (LD_{50} > 6180 mg *per os*).[145] **Ebselen** is a selenium-containing compound able to inhibit the activity of NDM-1 in a time- and concentration-dependent manner, suggesting a covalent reversible interaction with the enzyme. Mass spectrometer studies revealed the capability of **ebselen** to tightly bind NDM-1 *via* the formation of a covalent bond with Cys208 side-chain, disrupting the coordination with Zn2 that is consequently

removed from the active site (**Figure 24**). **Ebselen** is also able to reduce the MIC of ampicillin and MEM by 16- and 128-fold, respectively, thus restoring the activity of the two antibiotics on NDM-1 producing *E.coli* strains.[146] Recently, Jin *et al.* reported the successful structural optimization of **Ebselen,** through the generation of a library of forty-six 1,2-benzisoselenazol-3(2*H*)-one derivatives.[147] One of these compounds exhibited potent synergic activity with MEM against a panel of clinical NDM-1-producing Enterobacteriaceae isolates.

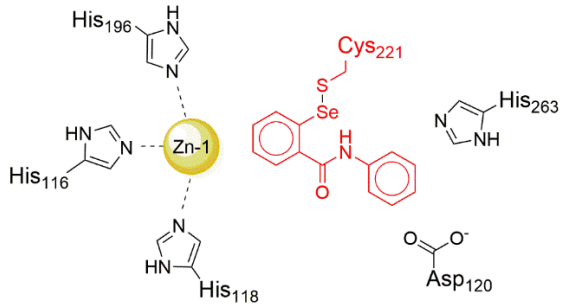

Figure 24. Covalent binding of Ebselen with Cys221 in NDM-1 active. Adapted with permission from Chiou, J.; Wan, S.; Chan, K. F.; So, P. K.; He, D.; Chan, E. W. C.; Chan, T. H.; Wong, K. Y.; Tao, J.; Chen, S. Ebselen as a Potent Covalent Inhibitor of New Delhi Metallo-β-Lactamase (NDM-1). Chem. Commun. **2015**, 51 (46), 9543–9546. Copyright 2015 Royal Chemical Society.

Christopeit *et al.* identified, by surface plasmon resonance (SPR), a set of four fragments inhibiting both NDM-1 and VIM-2. Compound **25a,** 3-cyanochromone, resulted the best fragment targeting NDM-1 with a K_d of 181 μM.[148] The compound was modified in the 3-formyl-chromone derivative (**25b, Figure 23**),[149] which showed a strong time dependent IC_{50}, going from 200 μM with no incubation to 2 μM after a 10 min incubation. The covalent inhibition mode was confirmed and studied by mass spectrometry and mutagenesis, highlighting the involvement of Lys211 in the formation of a Schiff base with the aldehyde in position 3 of the chromone. Surprisingly, **25b** resulted a selective inhibitor of NDM-1, without showing any significant activity against VIM-2. The absence of Lys211 in VIM-2 avoids the capability of **25b** to covalent bind NDM-1, explaining its spectrum of activity.

Thomas *et al*. reported in 2013 the development of an effective high-throughput screening and counter screening assay that led to the identification of another NDM-1 covalent inhibitor targeting a conserved active-site cysteine. Starting form a library of 1280 compounds, ten NDM-1 inhibitors (**pCBM**, **nitroprusside** and **26a-h**) were identified. Only **pCBM** (p-chloromercuricbenzoic acid, **Figure 23**) and **nitroprusside** (**Figure 23**) were assessed as effective NDM-1 inhibitors.[150]

1.2. Other inhibitors

Beside the NDM-1 inhibitors described so far, other chemical scaffolds were identified as potential NDM-1 inhibitors during the last years.

Thakur *et al*. selected 35 natural compounds from various plant sources and whose antibacterial activity is well documented in literature. Combining docking simulations with *in vitro* assays, **nimbolide**, **margolone**, **margolonone**, **isomargolonone**, **acetyl aleuritolic acid** and **harmane** were identified, and deserve some interest in the development of potent inhibitors active against NDM-1 (*see Supporting Information*).[127]

Wang *et al*. reported the identification of new NDM-1 inhibitors (**27a-c, 28a-aq**) by multi-step virtual screening performed on a library of over 2 millions of drug-like compounds. Compounds **27a-c** showed low micromolar affinity vs NDM-1 **(Figure 25)**. In series 28, only compound **28x** resulted active against NDM-1 (**Figure 25**) . [126]

Shen *et al.,* found that thiophene-carboxylic acid derivatives (**29a-e, Figure 25**) possess modest NDM-1 inhibition potency but synergic activity in combination with MEM.[151]

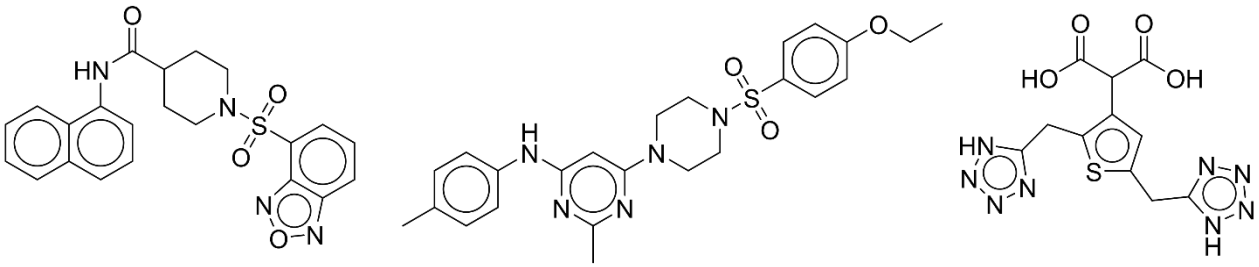

27c NDM-1 IC_{50} = 37.6 μM **28x** NDM-1 IC_{50} = 45.4 μM **29d** NDM-1 IC_{50} = 280 μM

Figure 25. Chemical structure and NDM-1 inhibitor activity of compounds **27c**, **28x** and **29d**.

Brindisi *et al.* reported a structure-based high throughput docking analysis on three MBLs (i.e. NDM-1, IMP-1 and VIM-2), looking for inhibitors active against multiple MBLs. The study led to the identification of **30a,** an aryl-methane-sulfonamide derivative linked to a quinoline ring by a hydrazine linker (**Figure 26Figure**). From docking calculations, **30a** is predicted to interact with the zinc ions though the methanesulfonamide moiety. The tricyclic system forms π–π interactions withTyr67 in VIM-2 and Phe70 in NDM-1, while the dioxole ring oxygen H-bonds Lys216. The chemical structure of **30a** was then modified at the zinc-bounding group, the dioxoquinoline ring and

the hydrazine linker. Derivatives **30b**, **30k**, **30l**, **30m**, **30o** and **30p** showed improved activity against VIM-2, whereas **30h**, **30n**, **30o** and **30v** were comparable to the lead compound **30a** (**Figure 26**).[68]

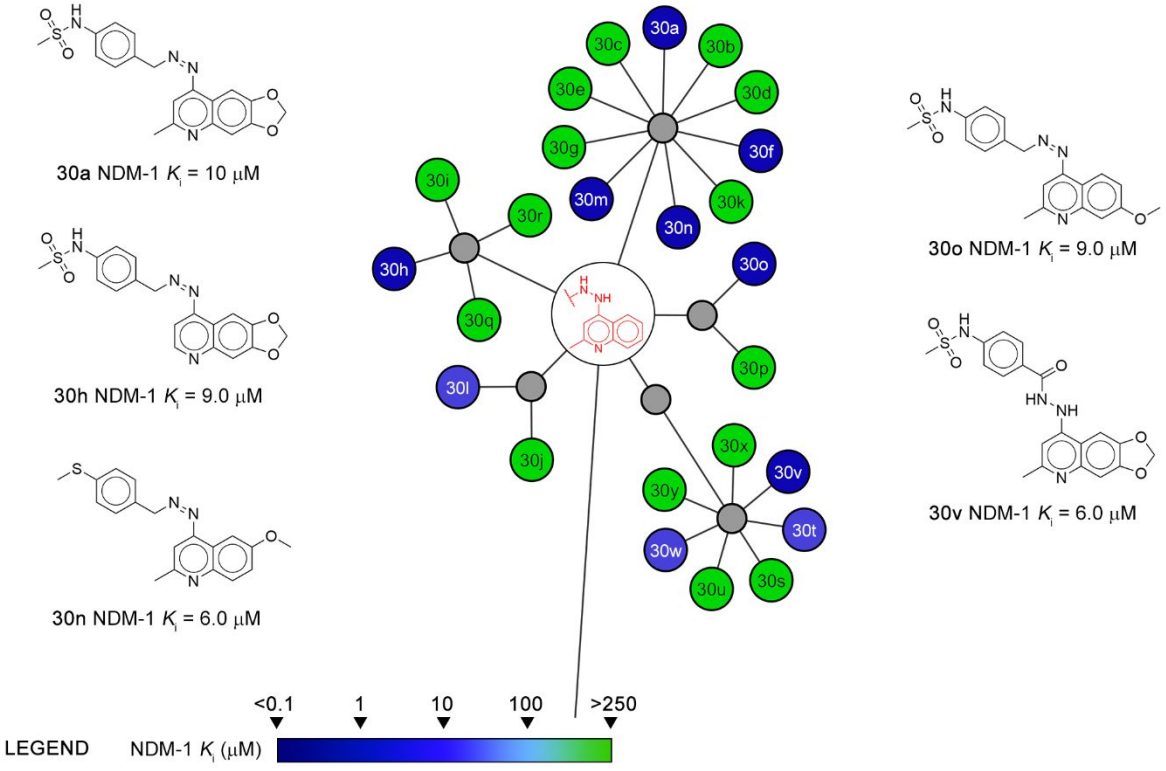

Figure 26. Chemical structure and NDM-1 enzymatic inhibitor activity of the most representative members of quinoline derivatives.

Khan *et al.* recently reported the discovery of novel non-β-lactam NDM-1 inhibitors by multistep virtual screening approach. Five chemical compounds (**31a-e**) with higher fitness score and binding energies were identified. The five compounds possess chemical features able to coordinate metal ions such as acylthiosemicarbazone (for **31a, Figure 27**), sulfonylacylazide (for **31b, Figure 27**) or sulfonylurea (for **31c, Figure 27**). The five compounds showed nanomolar IC_{50} against isolated NDM-1 and the capability of forming strong complexes with the enzyme. The MICs of the five inhibitors, in combination with ceftazidime, cefoxitin, MEM and IPM, were determined against *E.coli* NDM-1 expressing strains, revealing the ability for **31a-e** to synergize ceftazidime, cefoxitin and carbapenems.[67]

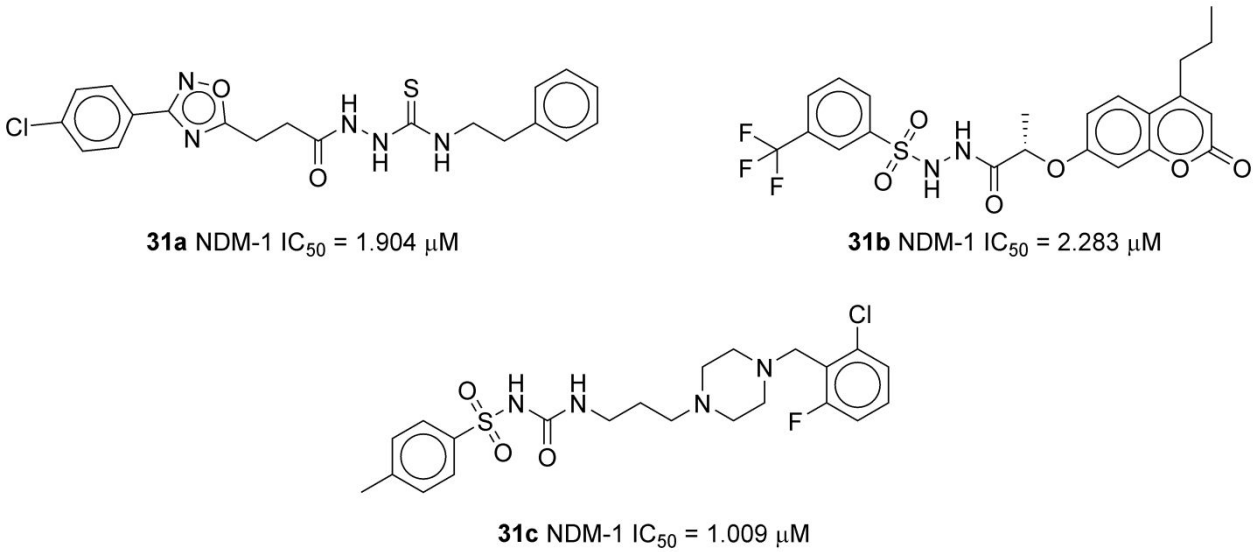

Figure 27. Chemical structure and NDM-1 enzymatic inhibitor activity of compounds **31a**, **b**, **c**.

Worthington *et al*. recently reported the identification of a 2-aminoimidazole able to effectively reduce the MIC of some antibiotics against multi-drug resistant *Acinetobacter baumanii* (MDRAB) and methicillin-resistant *Staphylococcus aureus* (MRSA), but showing low efficacy against *K. pneumoniae* NDM-1 producing strain.[152] A library of 2-aminoimidiazole analogues was screened for the capability to synergize IPM and MEM against a *K. pneumoniae* strain, and a first series of six aryl 2-aminoimidazole (**32a-f**) was identified. Analogues with linear alkyl substituents on the phenyl ring were found to be considerably more active, while the presence of butyl, t-butyl or phenyl substituents was detrimental. The lead compound **32d** (**Figure 28**) was able to reduce the MIC of both IPM and MEM by 16-fold at 30 μM, and by 256-fold at higher concentration. A second series of compounds substituted at position 4 and 5 was synthesized (**32g-n**). Only compound **32h** (**Figure 28**) was able to reduce the MIC of IPM and MEM by 8-fold, suggesting substitution at position 5 is unfavourable. Checkerboard assays of **32d** in combination with IPM and MEM confirmed the synergic activity. Further mechanistic studies are ongoing to confirm that the synergic effect is related to the inhibition of NDM-1.[153]

Recently, in March 2018, Everett *et al*. described the discovery of **ANT431** (**Figure 28**), a nanomolar, competitive inhibitor of NDM-1 and VIM-2. Biological studies performed on *E. coli* BL21(DE3) harbouring *bla*NDM-1 showed a strong potentiation of MEM antibacterial activity with a MIC reduction of 128-fold. The co-administration of 30 μg/mL of **ANT431** with MEM was able to restore bacteria susceptibility to the antibiotic in NDM-1 overexpressing isolates. **ANT431** showed a suitable pharmacokinetic profile for *in vivo* study, that is, high water solubility for intravenous administration,

good metabolic stability, moderate inhibition of CYP2C9 and CYP3A4 and no toxicity against human cell lines.[154]

Finally, Liu *et al*., screened 75 natural compounds against recombinant NDM-1, identifying **magnolol** (a natural compound isolated from magnolia bark) a potent inhibitor. **Magnolol** (**Figure 28**) inhibits NDM-1 enzyme activity with low micromolar affinity. The inhibitory activity is not affected by the supplement of zinc, suggesting that magnolol mode of action is not related to a metal-depletion mechanism. When administered in combination with MEM the compound was able to restore the antibiotic susceptibility in NDM-1expressing *E.coli* ZC-YN3 strain with a 4-fold MIC reduction (from 16 to 4 μg/mL).[155]

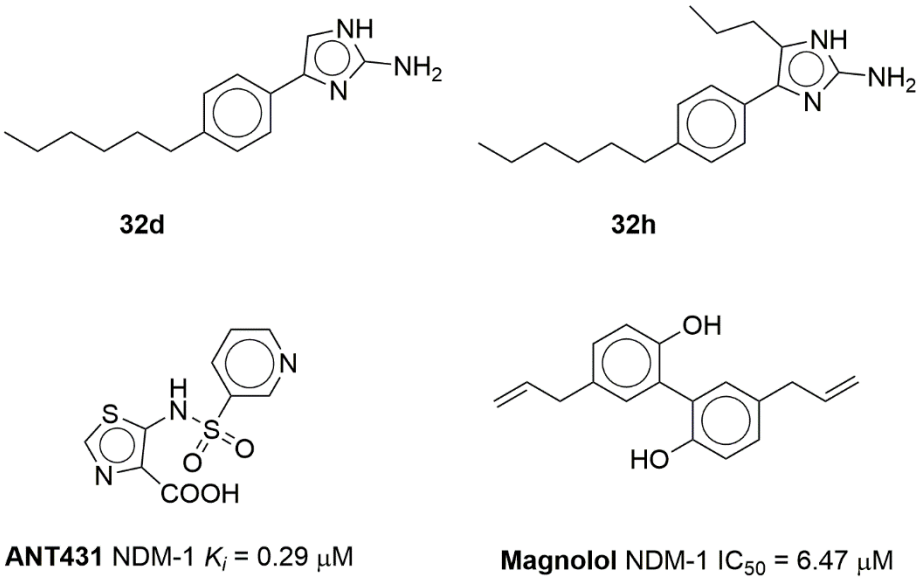

Figure 28. Chemical structure of compounds 32d,h, ANT431 and magnolol.

Conclusions

The discovery of a molecule able to restore the efficacy of available β-lactams toward resistant infections caused by NDM-1-expressing strains would have an enormous impact on human health and consistent social and economic returns. Unfortunately, despite the massive efforts dedicated over the years by many researchers all around the world, none of the new disclosed NDM-1 inhibitors has yet reached the clinic, and only a very few of them are currently under development.

Difficulties arise, primarily, from the nature of the protein itself and the related selectivity and toxicity issues, and from the variability in the mechanism by which β-lactams (penicillin, cephalosporins,

carbapenems) are hydrolyzed. As here described, coordinating the enzyme zinc ions bears the risk of inactivating essential human proteins as well, e.g. the metallo-proteases. Moreover, the flexibility of the enzyme, in terms of mutation rate and hydrolysis mechanism, promotes the development of resistant infections. This adaptability is also supported by a large and shallow active site, able to efficaciously orient almost any kind of β-lactam antibiotic. The design and development of molecules able to target this open cavity resulted actually quite difficult and often ineffective, in particular when structure-based drug design approaches are applied. The unexpected loop adjustment at the binding site entrance, the aforementioned flexibility of the pocket, as well as the water reorganization upon ligand binding make *in silico* prediction, as well as rational drug design strategies are often unreliable. A massive effort for the 3D resolution of the currently available inhibitor in NDM-1 active site is essential to develop new structure-based strategies and try to understand/predict the receptor flexibility. Apart from the difficulty to overcome selectivity issues and to properly fit such a large binding site, in fact, the clarification of the hydrolytic mechanism and of the binding mode of active inhibitors is crucial for the development of antibiotic less susceptible to the enzyme action or of more effective inhibitors.

At the moment, the most promising molecules share the presence of electron donor chemotypes able to coordinate the two metals, and of making hydrogen-bonds and/or salt bridges with the hydrogen bond donor residues of the binding site. Among these, the most common have mercapto-azolyl, aminotriazole, tetrazole, carboxylate, sulfonyl, and sulfonamide groups. However, recent findings on the evolution of NDM-1 variants coordinating Zn more tightly pose questions on how strategies involving the metal coordination can really counteract these enzymes. At the same time, the evidences of the ability of NDM-1, in light of its peculiar cellular localization, to resist to Zn depletion, open to new opportunities in bacterial targeting, i.e. enhancement of site-specific metal chelation elicited by the immune system and/or interference of bacterial lipidation.[19,156]

Particular attention must be deserved to the group of boronic acids derivatives: known to inhibit SBLs, they demonstrated to inactivate MBLs as well, mimicking the tetrahedral oxyanion formed during β-lactam hydrolysis and disrupting the active nucleophile in the binding site.[157] Currently, they represent a productive route toward broad-spectrum inhibitors, simultaneously inhibiting mechanistically different types of BLs.

We believe that only a strongly integrated effort, combining drug design strategies with a deeper understanding of the enzyme mechanism of action, and looking at new alternative/additional bacterial targets could lead to the identification of that key molecule or combination able to restore bacteria susceptibility to antibiotics.

Acknowledgments

Authors would like to thank Martina Montanari e Gian Marco Elisi for critical reading of the manuscript.

Associated content

Supporting Information

The supporting information is available free of charge on the ACS Publications website.

Table S1 reports the X-ray structures for apo and complexed NDM-1 available in the Protein Data Bank (PDF). S2_NDM-1 inhibitors.xls reports the code, SMILE, NDM-1 IC_{50} or K_i and DOI of the publication of each NDM-1 inhibitor discussed in the present review (XLS).

Author Information

Corresponding Authors

*E-mail: tondid@unimore.it (D.T.)

ORCID

Pasquale Linciano: 0000-0003-0382-7479

Donatella Tondi: 0000-0002-5195-5531

List of abbreviation

AMA, Aspergillomarasmine A; BL, β-Lactamase; BZT, bisthiazolidine; CcrA, metallo-β-lactamase from Bacteroides fragilis; CRE, carbapenem-resistant Enterobacteriaceae; DOTA, 1,4,7,10-tetraazacyclododecane-1,4,7,10-tetraacetic acid; DPA, 2,6-dipicolinic acid; ESBL, extended spectrum β-lactamase; EDTA, Ethylenediaminetetraacetic acid; FIC, Fractional inhibitory concentration; GES, Guiana Extended Spectrum; GIM-1, German imipenemase; IC_{50}, concentration inhibiting the 50% of the enzyme; ImiS, IMIpenem-hydrolysing β-lactamase-S; IMP, imipenemase; IPM, imipenem; K_i, inhibition constant; KPC, Klebsiella Pneumoniae Carbapenemase; MBL, Metallo β-Lactamase; MBP, 1-(2-mercaptobenzoyl)pyrrolidine-2-carboxylic acid; MDRAB, Multidrug-resistant Acinetobacter baumannii; MEM, meropenem; MIC, minimum inhibition concentration; MIF, Molecular Interaction Field; MRSA, Methicillin-Resistant Staphylococcus Aureus; NDM-1, New Delhi MBL-1; NOTA, 1,4,7-triazacyclononane-1,4,7-triacetic acid; PBP, penicillin binding proteins; pCBM, p-chloromercuricbenzoic acid; SAR, structure−activity relationship; SBL, serine based β-lactamase; SPR, surface plasmon resonance; VAB, vaborbactam; VIM, Verona integron-borne metallo-ß-lactamase.

Reference

(1) WHO. Antimicrobial Resistance. Global Report on Surveillance. *World Heal. Organ.* **2014**, *61* (3), 383–394 DOI: 10.1007/s13312-014-0374-3.

(2) World Health Organization. Global Action Plan on Antimicrobial Resistance. *WHO Press* **2015**, 166–173 DOI: 10.1016/j.cca.2016.09.023.

(3) Marrs, E. C. L.; Day, K. M.; Perry, J. D. In Vitro Activity of Mecillinam against Enterobacteriaceae with NDM-1 Carbapenemase. *J. Antimicrob. Chemother.* **2014**, *69* (10), 2873–2875 DOI: 10.1093/jac/dku204.

(4) Worthington, R. J.; Melander, C. Combination Approaches to Combat Multi-Drug Resistant. *Trends Biotechnol.* **2013**, *31* (3), 177–184 DOI: 10.1021/ac901991x.

(5) Potron, A.; Poirel, L.; Nordmann, P. Emerging Broad-Spectrum Resistance in Pseudomonas Aeruginosa and Acinetobacter Baumannii: Mechanisms and Epidemiology. *Int. J. Antimicrob. Agents* **2015**, *45* (6), 568–585 DOI: 10.1016/j.ijantimicag.2015.03.001.

(6) Khan, A. U.; Maryam, L.; Zarrilli, R. Structure, Genetics and Worldwide Spread of New Delhi Metallo-β-Lactamase (NDM): A Threat to Public Health. *BMC Microbiol.* **2017**, *17* (1), 1–12 DOI: 10.1186/s12866-017-1012-8.

(7) Hall, B. G.; Barlow, M. Revised Ambler Classification of β-Lactamases. *J. Antimicrob. Chemother.* **2005**, *55* (6), 1050–1051 DOI: 10.1093/jac/dki130.

(8) Bush, K.; Jacoby, G. A. Updated Functional Classification of β-Lactamases. *Antimicrob. Agents Chemother.* **2010**, *54* (3), 969–976 DOI: 10.1128/AAC.01009-09.

(9) Docquier, J. D. Mangani, S. Structure-Function Relationships of Class D Carbapenemases. *Curr Drug Targets* **2015**, *17* (9), 1061–1071 DOI: 10.2174/1389450116666150825115824.

(10) Jacoby, G. A. AmpC β-Lactamases. *Clin. Microbiol. Rev.* **2009**, *22* (1), 161–182 DOI: 10.1128/CMR.00036-08.

(11) Tondi, D.; Cross, S.; Venturelli, A.; Costi, M. P.; Cruciani, G.; Spyrakis, F. Decoding the Structural Basis For Carbapenem Hydrolysis By Class A Beta-Lactamases: Fishing For A Pharmacophore. *Curr. Drug Targets* **2016**, *17* (9), 983–1005 DOI: 10.2174/1389450116666151001104448.

(12) Mojica, M. F.; Bonomo, R. A.; Fast, W. B1-Metallo-β-Lactamases: Where Do We Stand? *Curr. Drugs Targets* **2016**, *17* (9), 1029–1050 DOI: 10.2174/1389450116666151001105622.

(13) Walsh, T. R.; Toleman, M. A.; Poirel, L. Metallo- β-Lactamases: The Quiet before the Storm? *Clin. Microbiol. Rev.* **2005**, *18* (2), 306–325 DOI: 10.1128/CMR.18.2.306.

(14) Bebrone, C. Metallo-β-Lactamases (Classification, Activity, Genetic Organization, Structure, Zinc Coordination) and Their Superfamily. *Biochem. Pharmacol.* **2007**, *74* (12), 1686–1701 DOI: 10.1016/j.bcp.2007.05.021.

(15) Queenan, A. M.; Bush, K. Carbapenemases: The Versatile β-Lactamases. *Clin. Microbiol. Rev.* **2007**, *20* (3), 440–458 DOI: 10.1128/CMR.00001-07.

(16) Bush, K.; Page, M. G. P. What We May Expect from Novel Antibacterial Agents in the Pipeline with Respect to Resistance and Pharmacodynamic Principles. *J. Pharmacokinet. Pharmacodyn.* **2017**, *44* (2), 113–132 DOI: 10.1007/s10928-017-9506-4.

(17) Palzkill, T. Metallo-β-Lactamase Structure and Function. *Ann. N. Y. Acad. Sci.* **2013**, *1277* (1), 91–104 DOI: 10.1111/j.1749-6632.2012.06796.x.

(18) Walsh, T. R.; Weeks, J.; Livermore, D. M.; Toleman, M. A. Dissemination of NDM-1 Positive Bacteria in the New Delhi Environment and Its Implications for Human Health: An Environmental Point Prevalence Study. *Lancet Infect. Dis.* **2011**, *11* (5), 355–362 DOI: 10.1016/S1473-3099(11)70059-7.

(19) Bahr, G.; Vitor-Horen, L.; Bethel, C. R.; Bonomo, R. A.; González, L. J.; Vila, A. J. Clinical Evolution of New Delhi Metallo-β-Lactamase (NDM) Optimizes Resistance under Zn(II) Deprivation. *Antimicrob. Agents Chemother.* **2018**, *62* (1) DOI: doi: 10.1128/AAC.01849-17.

(20) Yong, D.; Toleman, M. A.; Giske, C. G.; Cho, H. S.; Sundman, K.; Lee, K.; Walsh, T. R. Characterization of a New Metallo-β-Lactamase Gene, *Bla*NDM-1, and a Novel Erythromycin Esterase Gene Carried on a Unique Genetic Structure in Klebsiella Pneumoniae Sequence Type 14 from India. *Antimicrob. Agents Chemother.* **2009**, *53* (12), 5046–5054 DOI: 10.1128/AAC.00774-09.

(21) King, D. T.; Worrall, L. J.; Gruninger, R.; Strynadka, N. C. J. New Delhi Metallo-β-Lactamase: Structural Insights into β-Lactam Recognition and Inhibition. *J. Am. Chem. Soc.* **2012**, *134* (28), 11362–11365 DOI: 10.1021/ja303579d.

(22) Groundwater, P. W.; Xu, S.; Lai, F.; Váradi, L.; Tan, J.; Perry, J. D.; Hibbs, D. E. New Delhi Metallo-β-Lactamase-1: Structure, Inhibitors and Detection of Producers. *Future Med. Chem.* **2016**, *8* (9), 993–1012 DOI: 10.4155/fmc-2016-0015.

(23) Shaikh, S.; Fatima, J.; Shakil, S.; Rizvi, S. M. D.; Kamal, M. A. Antibiotic Resistance and Extended Spectrum Beta-Lactamases: Types, Epidemiology and Treatment. *Saudi J. Biol. Sci.* **2015**, *22* (1), 90–101 DOI: https://doi.org/10.1016/j.sjbs.2014.08.002.

(24) Supriya, U.; Shweta, M.; Malay, R. Sen; Amitabha, B. Role of Carbapenemases in Antibiotic Resistance of Gram Negative Organisms and Their Detection. **2012**, 101–124 DOI: 10.1002/sim.5442.

(25) Rolain, J. M.; Parola, P.; Cornaglia, G. New Delhi Metallo-β-Lactamase (NDM-1): Towards a New Pandemia? *Clin. Microbiol. Infect.* **2010**, *16* (12), 1699–1701 DOI: 10.1111/j.1469-0691.2010.03385.x.

(26) Nordmann, P.; Poirel, L.; Walsh, T. R.; Livermore, D. M. The Emerging NDM Carbapenemases. *Trends Microbiol.* **2011**, *19* (12), 588–595 DOI: 10.1016/j.tim.2011.09.005.

(27) Nordmann, P.; Gniadkowski, M.; Giske, C. G.; Poirel, L.; Woodford, N.; Miriagou, V.; Akova, M.; Naas, T.; Seifert, H.; Livermore, D.; et al. Identification and Screening of Carbapenemase-Producing Enterobacteriaceae. *Clin. Microbiol. Infect.* **2012**, *18* (5), 432–438 DOI: 10.1111/j.1469-0691.2012.03815.x.

(28) Nordmann, P.; Boulanger, A. E.; Poirel, L. NDM-4 Metallo-β-Lactamase with Increased Carbapenemase Activity from Escherichia Coli. *Antimicrob. Agents Chemother.* **2012**, *56* (4), 2184–2186 DOI: 10.1128/AAC.05961-11.

(29) Carattoli, A.; Seiffert, S. N.; Schwendener, S.; Perreten, V.; Endimiani, A. Differentiation of IncL and IncM Plasmids Associated with the Spread of Clinically Relevant Antimicrobial Resistance. *PLoS One* **2015**, *10* (5), e0123063 DOI: 10.1371/journal.pone.0123063.

(30) Rogers, B. A.; Sidjabat, H. E.; Silvey, A.; Anderson, T. L.; Perera, S.; Li, J.; Paterson, D. L. Treatment Options for New Delhi Metallo-β-Lactamase-Harboring Enterobacteriaceae. *Microb. Drug Resist.* **2013**, *19* (2), 100–103 DOI: 10.1089/mdr.2012.0063.

(31) Zhang, H.; Hao, Q. Crystal Structure of NDM-1 Reveals a Common β-Lactam Hydrolysis Mechanism. *FASEB J.* **2011**, *25* (8), 2574–2582 DOI: 10.1096/fj.11-184036.

(32) King, D.; Strynadka, N. Crystal Structure of New Delhi Metallo-β-Lactamase Reveals Molecular Basis for Antibiotic Resistance. *Protein Sci.* **2011**, *20* (9), 1484–1491 DOI: 10.1002/pro.697.

(33) Kim, Y.; Tesar, C.; Mire, J.; Jedrzejczak, R.; Binkowski, A.; Babnigg, G.; Sacchettini, J.; Joachimiak, A. Structure of Apo- and Monometalated Forms of NDM-1-A Highly Potent Carbapenem-Hydrolyzing Metallo-β-Lactamase. *PLoS One* **2011**, *6* (9), e24621 DOI: 10.1371/journal.pone.0024621.

(34) Lassaux, P.; Traoré, D. A. K.; Loisel, E.; Favier, A.; Docquier, J. D.; Sohier, J. S.; Laurent, C.; Bebrone, C.; Frère, J. M.; Ferrer, J. L.; et al. Biochemical and Structural Characterization of the Subclass B1 Metallo-β-Lactamase VIM-4. *Antimicrob. Agents Chemother.* **2011**, *55* (3), 1248–1255 DOI: 10.1128/AAC.01486-09.

(35) Lisa, M. N.; Palacios, A. R.; Aitha, M.; González, M. M.; Moreno, Di. M.; Crowder, M. W.; Bonomo, R. A.; Spencer, J.; Tierney, D. L.; Llarrull, L. I.; et al. A General Reaction

Mechanism for Carbapenem Hydrolysis by Mononuclear and Binuclear Metallo-β-Lactamases. *Nat. Commun.* **2017**, *8* (1) DOI: 10.1038/s41467-017-00601-9.

(36) Feng, H.; Ding, J.; Zhu, D.; Liu, X.; Xu, X.; Zhang, Y.; Zang, S.; Wang, D. C.; Liu, W. Structural and Mechanistic Insights into NDM-1 Catalyzed Hydrolysis of Cephalosporins. *J. Am. Chem. Soc.* **2014**, *136* (42), 14694–14697 DOI: 10.1021/ja508388e.

(37) Zheng, M.; Xu, D. New Delhi Metallo-β-Lactamase 1: Substrate Binding and Catalytic Mechanism. *J. Phys. Chem. B* **2013**, *117* (39), 11596–11607 DOI: 10.1021/jp4065906.

(38) Kim, Y.; Cunningham, M. A.; Mire, J.; Tesar, C.; Sacchettini, J.; Joachimiak, A. NDM-1, the Ultimate Promiscuous Enzyme: Substrate Recognition and Catalytic Mechanism. *FASEB J.* **2013**, *27* (5), 1917–1927 DOI: 10.1096/fj.12-224014.

(39) Yang, H.; Young, H.; Yu, S.; Sutton, L.; Crowder, M. W. Targeting Metallo-Carbapenemases via Modulation of Electronic Properties of Cephalosporins. *Biochem. J.* **2014**, *464* (2), 271–279 DOI: 10.1042/BJ20140364.

(40) Farina, D.; Spyrakis, F.; Venturelli, A.; Cross, S.; Tondi, D.; Costi, M. P. The Inhibition of Extended Spectrum Beta-Lactamases: Hits and Leads. *Curr. Med. Chem.* **2014**, *21* (12), 1405–1434 DOI: 10.2174/09298673113206660323.

(41) Yang, H.; Aitha, M.; Hetrick, A. M.; Richmond, T. K.; Tierney, D. L.; Crowder, M. W. Mechanistic and Spectroscopic Studies of Metallo-β-Lactamase NDM-1. *Biochemistry* **2012**, *51* (18), 3839–3847 DOI: 10.1021/bi300056y.

(42) Aitha, M.; Moller, A. J.; Sahu, I. D.; Horitani, M.; Tierney, D. L.; Crowder, M. W. Investigating the Position of the Hairpin Loop in New Delhi Metallo-β-Lactamase, NDM-1, during Catalysis and Inhibitor Binding. *J. Inorg. Biochem.* **2016**, *156*, 35–39 DOI: 10.1016/j.jinorgbio.2015.10.011.

(43) Yang, H.; Aitha, M.; Marts, A. R.; Hetrick, A.; Bennett, B.; Crowder, M. W.; Tierney, D. L. Spectroscopic and Mechanistic Studies of Heterodimetallic Forms of Metallo-β-Lactamase NDM-1. *J. Am. Chem. Soc.* **2014**, *136* (20), 7273–7285 DOI: 10.1021/ja410376s.

(44) Zhang, H.; Hao, Q. Crystal Structure of NDM-1 Reveals a Common β-Lactam Hydrolysis Mechanism. *FASEB J.* **2011**, *25* (8), 2574–2582 DOI: 10.1096/fj.11-184036.

(45) Concha, N. O.; Rasmussen, B. A.; Bush, K.; Herzberg, O. Crystal Structure of the Wide-Spectrum Binuclear Zinc β- Lactamase from Bacteroides Fragilis. *Structure* **1996**, *4* (7), 823–836 DOI: 10.1016/S0969-2126(96)00089-5.

(46) Simona, F.; Magistrato, A.; Dal Peraro, M.; Cavalli, A.; Vila, A. J.; Carloni, P. Common Mechanistic Features among Metallo-β-Lactamases: A Computational Study of Aeromonas Hydrophila CphA Enzyme. *J. Biol. Chem.* **2009**, *284* (41), 28164–28171 DOI:

10.1074/jbc.M109.049502.

(47) Feng, H.; Liu, X.; Wang, S.; Fleming, J.; Wang, D. C.; Liu, W. The Mechanism of NDM-1-Catalyzed Carbapenem Hydrolysis Is Distinct from That of Penicillin or Cephalosporin Hydrolysis. *Nat. Commun.* **2017**, *8* (1) DOI: 10.1038/s41467-017-02339-w.

(48) King, D. T.; Strynadka, N. C. J. Targeting Metallo-β-Lactamase Enzymes in Antibiotic Resistance. *Future Med. Chem.* **2013**, *5* (11), 1243–1263 DOI: 10.4155/fmc.13.55.

(49) Baroni, M.; Cruciani, G.; Sciabola, S.; Perruccio, F.; Mason, J. S. A Common Reference Framework for Analyzing/Comparing Proteins and Ligands. Fingerprints for Ligands and Proteins (FLAP): Theory and Application. *J. Chem. Inf. Model.* **2007**, *47* (2), 279–294 DOI: 10.1021/ci600253e.

(50) Spyrakis, F.; Benedetti, P.; Decherchi, S.; Rocchia, W.; Cavalli, A.; Alcaro, S.; Ortuso, F.; Baroni, M.; Cruciani, G. A Pipeline To Enhance Ligand Virtual Screening: Integrating Molecular Dynamics and Fingerprints for Ligand and Proteins. *J. Chem. Inf. Model.* **2015**, *55* (10), 2256–2274 DOI: 10.1021/acs.jcim.5b00169.

(51) Drawz, S. M.; Bonomo, R. A. Three Decades of β-Lactamase Inhibitors. *Clin. Microbiol. Rev.* **2010**, *23* (1), 160–201 DOI: 10.1128/CMR.00037-09.

(52) Page, S.; Song, H.; Wu, D. C. Assessing the Impacts of the Global Economic Crisis and Swine Flu on Inbound Tourism Demand in the United Kingdom. *J. Travel Res.* **2012**, *51* (2), 142–153 DOI: 10.1177/0047287511400754.

(53) Van den Akker, F.; Bonomo, R. A. Exploring Additional Dimensions of Complexity in Inhibitor Design for Serine β-Lactamases: Mechanistic and Intra- and Inter-Molecular Chemistry Approaches. *Front. Microbiol.* **2018**, *9*, 622 DOI: 10.3389/fmicb.2018.00622.

(54) Celenza, G.; Vicario, M.; Bellio, P.; Linciano, P.; Perilli, M.; Oliver, A.; Blazquez, J.; Cendron, L.; Tondi, D. Phenylboronic Acid Derivatives as Validated Leads Active in Clinical Strains Overexpressing KPC-2: A Step against Bacterial Resistance. *ChemMedChem* **2018** DOI: 10.1002/cmdc.201700788.

(55) Klein, R.; Linciano, P.; Celenza, G.; Bellio, P.; Papaioannou, S.; Blazquez, J.; Cendron, L.; Brenk, R.; Tondi, D. In Silico Identification and In Vitro Validation of Novel KPC-2 β-Lactamase Inhibitors. *bioRxiv* **2018**.

(56) Tondi, D.; Venturelli, A.; Bonnet, R.; Pozzi, C.; Shoichet, B. K.; Costi, M. P. Targeting Class A and C Serine β-Lactamases with a Broad-Spectrum Boronic Acid Derivative. *J. Med. Chem.* **2014**, *57* (12), 5449–5458 DOI: 10.1021/jm5006572.

(57) Genovese, F.; Lazzari, S.; Venturi, E.; Costantino, L.; Blazquez, J.; Ibacache-Quiroga, C.; Costi, M. P.; Tondi, D. Design, Synthesis and Biological Evaluation of Non-Covalent AmpC

β-Lactamases Inhibitors. *Med. Chem. Res.* **2017**, *26* (5), 975–986 DOI: 10.1007/s00044-017-1809-x.

(58) Eidam, O.; Romagnoli, C.; Dalmasso, G.; Barelier, S.; Caselli, E.; Bonnet, R.; Shoichet, B. K.; Prati, F. Fragment-Guided Design of Subnanomolar β-Lactamase Inhibitors Active in Vivo. *Proc. Natl. Acad. Sci.* **2012**, *109* (43), 17448–17453 DOI: 10.1073/pnas.1208337109.

(59) Khan, A.; Faheem, M.; Danishuddin, M.; Khan, A. U. Evaluation of Inhibitory Action of Novel Non β-Lactam Inhibitor against Klebsiella Pneumoniae Carbapenemase (KPC-2). *PLoS One* **2014**, *9* (9), e108246.

(60) Kaase, M.; Nordmann, P.; Wichelhaus, T. A.; Gatermann, S. G.; Bonnin, R. A.; Poirel, L. NDM-2 Carbapenemase in Acinetobacter Baumannii from Egypt. *J. Antimicrob. Chemother.* **2011**, *66* (6), 1260–1262 DOI: 10.1093/jac/dkr135.

(61) Khan, A. U.; Nordmann, P. Spread of Carbapenemase NDM-1 Producers: The Situation in India and What May Be Proposed. *Scand. J. Infect. Dis.* **2012**, *44* (7), 531–535 DOI: 10.3109/00365548.2012.669046.

(62) Rahman, M.; Shukla, S. K.; Prasad, K. N.; Ovejero, C. M.; Pati, B. K.; Tripathi, A.; Singh, A.; Srivastava, A. K.; Gonzalez-Zorn, B. Prevalence and Molecular Characterisation of New Delhi Metallo-β- Lactamases NDM-1, NDM-5, NDM-6 and NDM-7 in Multidrug-Resistant Enterobacteriaceae from India. *Int. J. Antimicrob. Agents* **2014**, *44* (1), 30–37 DOI: 10.1016/j.ijantimicag.2014.03.003.

(63) Liu, Z.; Li, J.; Wang, X.; Liu, D.; Ke, Y.; Wang, Y.; Shen, J. Novel Variant of New Delhi Metallo-β-Lactamase, NDM-20, in Escherichia Coli. *Front. Microbiol.* **2018**, *9*, 248 DOI: 10.3389/fmicb.2018.00248.

(64) Mojica, M. F.; Bonomo, R. A.; Fast, W. B1-Metallo-Beta-Lactamases:Where Do We Stand? *Curr. Drug Targets* **2016**, *17* (9), 1029–1050 DOI: 10.1111/conl.12303.

(65) Zou, D.; Huang, Y.; Zhao, X.; Liu, W.; Dong, D.; Li, H.; Wang, X.; Huang, S.; Wei, X.; Yan, X.; et al. A Novel New Delhi Metallo-β-Lactamase Variant, NDM-14, Isolated in a Chinese Hospital Possesses Increased Enzymatic Activity against Carbapenems. *Antimicrob. Agents Chemother.* **2015**, *59* (4), 2450–2453 DOI: 10.1128/AAC.05168-14.

(66) Klingler, F. M.; Moser, D.; Büttner, D.; Wichelhaus, T. A.; Löhr, F.; Dötsch, V.; Proschak, E. Probing Metallo-β-Lactamases with Molecular Fragments Identified by Consensus Docking. *Bioorganic Med. Chem. Lett.* **2015**, *25* (22), 5243–5246 DOI: 10.1016/j.bmcl.2015.09.056.

(67) Khan, A. U.; Ali, A.; Danishuddin, D.; Srivastava, G.; Sharma, A. Potential Inhibitors Designed against NDM-1 Type Metallo-β-Lactamases: An Attempt to Enhance Efficacies of

Antibiotics against Multi-Drug-Resistant Bacteria. *Sci. Rep.* **2017**, *7* (1), 1–14 DOI: 10.1038/s41598-017-09588-1.

(68) Brindisi, M.; Brogi, S.; Giovani, S.; Gemma, S.; Lamponi, S.; De Luca, F.; Novellino, E.; Campiani, G.; Docquier, J. D.; Butini, S. Targeting Clinically-Relevant Metallo-β-Lactamases: From High-Throughput Docking to Broad-Spectrum Inhibitors. *J. Enzyme Inhib. Med. Chem.* **2016**, *31*, 98–109 DOI: 10.3109/14756366.2016.1172575.

(69) Meini, M.-R.; Llarrull, L. I.; Vila, A. J. Overcoming Differences: The Catalytic Mechanism of Metallo-Beta-Lactamases. *FEBS Lett.* **2015**, *589* (22), 3419–3432 DOI: 10.1016/j.febslet.2015.08.015.

(70) Rogers, D.; Hahn, M. Extended-Connectivity Fingerprints. *J. Chem. Inf. Model.* **2010**, *50* (5), 742–754 DOI: 10.1021/ci100050t.

(71) Bajusz, D.; Rácz, A.; Héberger, K. Why Is Tanimoto Index an Appropriate Choice for Fingerprint-Based Similarity Calculations? *J. Cheminform.* **2015**, *7* (1), 20–25 DOI: 10.1186/s13321-015-0069-3.

(72) Shannon, P.; Markiel, A.; Ozier, O.; Baliga, N. S.; Wang, J. T.; Ramage, D.; Amin, N.; Schwikowski, B.; Ideker, T. Cytoscape: A Software Environment for Integrated Models of Biomolecular Interaction Networks. *Genome Res.* **2003**, *13* (11), 2498–2504 DOI: 10.1101/gr.1239303.

(73) Buckley, L. M.; Mcewan, N. A.; Nuttall, T. Tris-EDTA Significantly Enhances Antibiotic Efficacy against Multidrug-Resistant Pseudomonas Aeruginosa in Vitro. *Vet. Dermatol.* **2013**, *24* (5), 519-e122 DOI: 10.1111/vde.12071.

(74) Lambert, R. J. W.; Hanlon, G. W.; Denyer, S. P. The Synergistic Effect of EDTA/Antimicrobial Combinations on Pseudomonas Aeruginosa. *J. Appl. Microbiol.* **2004**, *96* (2), 244–253 DOI: 10.1046/j.1365-2672.2004.02135.x.

(75) Amaral, K. F.; Rogero, M. M.; Fock, R. A.; Borelli, P.; Gavini, G. Cytotoxicity Analysis of EDTA and Citric Acid Applied on Murine Resident Macrophages Culture. *Int. Endod. J.* **2007**, *40* (5), 338–343 DOI: 10.1111/j.1365-2591.2007.01220.x.

(76) Lin-Tan, D. T.; Lin, J. L.; Yen, T. H.; Chen, K. H.; Huang, Y. L. Long-Term Outcome of Repeated Lead Chelation Therapy in Progressive Non-Diabetic Chronic Kidney Diseases. *Nephrol. Dial. Transplant.* **2007**, *22* (10), 2924–2931 DOI: 10.1093/ndt/gfm342.

(77) Aoki, N.; Ishii, Y.; Tateda, K.; Saga, T.; Kimura, S.; Kikuchi, Y.; Kobayashi, T.; Tanabe, Y.; Tsukada, H.; Gejyo, F.; et al. Efficacy of Calcium-EDTA as an Inhibitor for Metallo-β-Lactamase in a Mouse Model of Pseudomonas Aeruginosa Pneumonia. *Antimicrob. Agents Chemother.* **2010**, *54* (11), 4582–4588 DOI: 10.1128/AAC.00511-10.

(78) Yoshizumi, A.; Ishii, Y.; Livermore, D. M.; Woodford, N.; Kimura, S.; Saga, T.; Harada, S.; Yamaguchi, K.; Tateda, K. Efficacies of Calcium-EDTA in Combination with Imipenem in a Murine Model of Sepsis Caused by Escherichia Coli with NDM-1 β-Lactamase. *J. Infect. Chemother.* **2013**, *19* (5), 992–995 DOI: 10.1007/s10156-012-0528-y.

(79) Haenni, A. L.; Robert, M.; Vetter, W.; Roux, L.; Barbier, M.; Lederer, E. Structure Chimique Des Aspergillomarasmines A et B. *Helv. Chim. Acta* **1965**, *48* (4), 729–750 DOI: 10.1002/hlca.19650480409.

(80) Mikami, Y.; Suzuki, T. Novel Microbial Inhibitors of Angiotensin-Converting Enzyme, Aspergillomarasmines A and B. *Agric. Biol. Chem.* **1983**, *47* (11), 2693–2695 DOI: 10.1271/bbb1961.47.2693.

(81) King, A. M.; Reid-Yu, S. A.; Wang, W.; King, D. T.; De Pascale, G.; Strynadka, N. C.; Walsh, T. R.; Coombes, B. K.; Wright, G. D. Aspergillomarasmine A Overcomes Metallo-β-Lactamase Antibiotic Resistance. *Nature* **2014**, *510* (7506), 503–506 DOI: 10.1038/nature13445.

(82) Bergstrom, A.; Katko, A.; Adkins, Z.; Hill, J.; Cheng, Z.; Burnett, M.; Yang, H.; Aitha, M.; Mehaffey, M. R.; Brodbelt, J. S.; et al. Probing the Interaction of Aspergillomarasmine A with Metallo-β-Lactamases NDM-1, VIM-2, and IMP-7. *ACS Infect. Dis.* **2018**, *4* (2), 135–145 DOI: 10.1021/acsinfecdis.7b00106.

(83) Paul-soto, R.; Bauer, R.; Frère, J.; Galleni, M.; Meyer-klaucke, W.; Nolting, H.; Rossolini, G. M.; Seny, D. De; Hernandez-valladares, M.; Zeppezauer, M.; et al. Mono- and Binuclear Zn 2+-β-Lactamase. *J. Biol. Chem.* **1999**, *274* (19), 13242–13249 DOI: 10.1074/jbc.274.19.13242.

(84) Friis, P.; Olsen, C. E.; Møller, B. L. Toxin Production in Pyrenophora Teres, the Ascomycete Causing the Net-Spot Blotch Disease of Barley (Hordeum Vulgare L.). *J. Biol. Chem.* **1991**, *266* (20), 13329–13335.

(85) Liao, D.; Yang, S.; Wang, J.; Zhang, J.; Hong, B.; Wu, F.; Lei, X. Total Synthesis and Structural Reassignment of Aspergillomarasmine A. *Angew. Chemie - Int. Ed.* **2016**, *55* (13), 4291–4295 DOI: 10.1002/anie.201509960.

(86) Koteva, K.; King, A. M.; Capretta, A.; Wright, G. D. Total Synthesis and Activity of the Metallo-β-Lactamase Inhibitor Aspergillomarasmine A. *Angew. Chemie Int. Ed.* **2016**, *55* (6), 2210–2212 DOI: 10.1002/anie.201510057.

(87) Zhang, J.; Wang, S.; Wei, Q.; Guo, Q.; Bai, Y.; Yang, S.; Song, F.; Zhang, L.; Lei, X. Synthesis and Biological Evaluation of Aspergillomarasmine A Derivatives as Novel NDM-1 Inhibitor to Overcome Antibiotics Resistance. *Bioorganic Med. Chem.* **2017**, *25* (19),

5133–5141 DOI: 10.1016/j.bmc.2017.07.025.

(88) Docquier, J. D.; Lamotte-Brasseur, J.; Galleni, M.; Amicosante, G.; Frère, J. M.; Rossolini, G. M. On Functional and Structural Heterogeneity of VIM-Type Metallo-β-Lactamases. *J. Antimicrob. Chemother.* **2003**, *51* (2), 257–266 DOI: 10.1093/jac/dkg067.

(89) Somboro, A. M.; Tiwari, D.; Bester, L. A.; Parboosing, R.; Chonco, L.; Kruger, H. G.; Arvidsson, P. I.; Govender, T.; Naicker, T.; Essack, S. Y. NOTA: A Potent Metallo-β-Lactamase Inhibitor. *J. Antimicrob. Chemother.* **2014**, *70* (5), 1594–1596 DOI: 10.1093/jac/dku538.

(90) Livermore, D. M.; Mushtaq, S.; Morinaka, A.; Ida, T.; Maebashi, K.; Hope, R. Activity of Carbapenems with ME1071 (Disodium 2,3-Diethylmaleate) against Enterobacteriaceae and Acinetobacter Spp. With Carbapenemases, Including NDM Enzymes. *J. Antimicrob. Chemother.* **2013**, *68* (1), 153–158 DOI: 10.1093/jac/dks350.

(91) Schnaars, C.; Kildahl-Andersen, G.; Prandina, A.; Popal, R.; Radix, S. L.; Le Borgne, M.; Gjoen, T.; Andresen, A. M. S.; Heikal, A.; Økstad, O. A.; et al. Synthesis and Preclinical Evaluation of TPA-Based Zinc Chelators as Metallo-β-Lactamase Inhibitors. *ACS Infect. Dis.* **2018** DOI: 10.1021/acsinfecdis.8b00137.

(92) Brunton, L.; Chabner, B.; Knollman, B. *Goodman and Gilman's The Pharmacological Basis of Therapeutics*, 12th ed.; McGraw Hill Medical, 2013.

(93) Yusof, Y.; Tan, D. T. C.; Arjomandi, O. K.; Schenk, G.; McGeary, R. P. Captopril Analogues as Metallo-β-Lactamase Inhibitors. *Bioorganic Med. Chem. Lett.* **2016**, *26* (6), 1589–1593 DOI: 10.1016/j.bmcl.2016.02.007.

(94) Liénard, B. M. R.; Garau, G.; Horsfall, L.; Karsisiotis, A. I.; Damblon, C.; Lassaux, P.; Papamicael, C.; Roberts, G. C. K.; Galleni, M.; Dideberg, O.; et al. Structural Basis for the Broad-Spectrum Inhibition of Metallo-β-Lactamases by Thiols. *Org. Biomol. Chem.* **2008**, *6* (13), 2282–2294 DOI: 10.1039/B802311E.

(95) Tehrani, K. H. M. E.; Martin, N. I. Thiol-Containing Metallo-β-Lactamase Inhibitors Resensitize Resistant Gram-Negative Bacteria to Meropenem. *ACS Infect. Dis.* **2017**, *3* (10), 711–717 DOI: 10.1021/acsinfecdis.7b00094.

(96) Guo, Y.; Wang, J.; Niu, G.; Shui, W.; Sun, Y.; Zhou, H.; Zhang, Y.; Yang, C.; Lou, Z.; Rao, Z. A Structural View of the Antibiotic Degradation Enzyme NDM-1 from a Superbug. *Protein Cell* **2011**, *2* (5), 384–394 DOI: 10.1007/s13238-011-1055-9.

(97) García-Sáez, I.; Hopkins, J.; Papamicael, C.; Franceschini, N.; Amicosante, G.; Rossolinill, G. M.; Galleni, M.; Frère, J. M.; Dideberg, O. The 1.5-Å Structure of Chryseobacterium Meningosepticum Zinc β-Lactamase in Complex with the Inhibitor, D-Captopril. *J. Biol.*

Chem. **2003**, *278* (26), 23868–23873 DOI: 10.1074/jbc.M301062200.

(98) Kim, Y.; Tesar, C.; Jedrzejczak, R.; Babnigg, J.; Mire, J.; Sacchettini, J.; Joachimiak, A. New Delhi Metallo-β-Lactamase-1 1.05 Å Structure Complexed with Hydrolyzed Ampicillin. *Protein Data Bank* **2012** DOI: 10.2210/PDB4HL2/PDB.

(99) Brem, J.; Van Berkel, S. S.; Zollman, D.; Lee, S. Y.; Gileadi, O.; McHugh, P. J.; Walsh, T. R.; McDonough, Michael A. Schofield, C. J. Structural Basis of Metallo- β -Lactamase Inhibition by Captopril Stereoisomers. *Am. Soc. Microbiol.* **2016**, *60* (1), 142–150 DOI: 10.1128/AAC.01335-15.

(100) Antony, J.; Gresh, N.; Olsen, L.; Hemmingsen, L.; Schofield, C. J.; Bauer, R. Binding of D- and L-Captopril Inhibitors to Metallo-β-Lactamase Studied by Polarizable Molecular Mechanics and Quantum Mechanics. *J. Comput. Chem.* **2002**, *23* (13), 1281–1296 DOI: 10.1002/jcc.10111.

(101) Klingler, F. M.; Wichelhaus, T. A.; Frank, D.; Cuesta-Bernal, J.; El-Delik, J.; Müller, H. F.; Sjuts, H.; Göttig, S.; Koenigs, A.; Pos, K. M.; et al. Approved Drugs Containing Thiols as Inhibitors of Metallo-β-Lactamases: Strategy to Combat Multidrug-Resistant Bacteria. *J. Med. Chem.* **2015**, *58* (8), 3626–3630 DOI: 10.1021/jm501844d.

(102) Klingler, F. M.; Wichelhaus, T. A.; Frank, D.; Cuesta-Bernal, J.; El-Delik, J.; Müller, H. F.; Sjuts, H.; Göttig, S.; Koenigs, A.; Pos, K. M.; et al. Approved Drugs Containing Thiols as Inhibitors of Metallo-β-Lactamases: Strategy to Combat Multidrug-Resistant Bacteria. *J. Med. Chem.* **2015**, *58* (8), 3626–3630 DOI: 10.1021/jm501844d.

(103) Li, N.; Xu, Y.; Xia, Q.; Bai, C.; Wang, T.; Wang, L.; He, D.; Xie, N.; Li, L.; Wang, J.; et al. Simplified Captopril Analogues as NDM-1 Inhibitors. *Bioorganic Med. Chem. Lett.* **2014**, *24* (1), 386–389 DOI: 10.1016/j.bmcl.2013.10.068.

(104) Büttner, D.; Kramer, J. S.; Klingler, F. M.; Wittmann, S. K.; Hartmann, M. R.; Kurz, C. G.; Kohnhäuser, D.; Weizel, L.; Brüggerhoff, A.; Frank, D.; et al. Challenges in the Development of a Thiol-Based Broad-Spectrum Inhibitor for Metallo-β-Lactamases. *ACS Infect. Dis.* **2018**, *4* (3), 360–372 DOI: 10.1021/acsinfecdis.7b00129.

(105) Chen, X.; Li, L.; Chen, S.; Xu, Y.; Xia, Q.; Guo, Y.; Liu, X.; Tang, Y.; Zhang, T.; Chen, Y.; et al. Identification of Inhibitors of the Antibiotic-Resistance Target New Delhi Metallo-β-Lactamase 1 by Both Nanoelectrospray Ionization Mass Spectrometry and Ultrafiltration Liquid Chromatography/Mass Spectrometry Approaches. *Anal. Chem.* **2013**, *85* (16), 7957–7965 DOI: 10.1021/ac401732d.

(106) Ma, J.; Cao, Q.; McLeod, S. M.; Ferguson, K.; Gao, N.; Breeze, A. L.; Hu, J. Target-Based Whole-Cell Screening By1H NMR Spectroscopy. *Angew. Chemie - Int. Ed.* **2015**, *54* (16),

4764–4767 DOI: 10.1002/anie.201410701.

(107) Liu, X. L.; Shi, Y.; Kang, J. S.; Oelschlaeger, P.; Yang, K. W. Amino Acid Thioester Derivatives: A Highly Promising Scaffold for the Development of Metallo-β-Lactamase L1 Inhibitors. *ACS Med. Chem. Lett.* **2015**, *6* (6), 660–664 DOI: 10.1021/acsmedchemlett.5b00098.

(108) Liu, S.; Jing, L.; Yu, Z. J.; Wu, C.; Zheng, Y.; Zhang, E.; Chen, Q.; Yu, Y.; Guo, L.; Wu, Y.; et al. ((S)-3-Mercapto-2-Methylpropanamido)Acetic Acid Derivatives as Metallo-β-Lactamase Inhibitors: Synthesis, Kinetic and Crystallographic Studies. *Eur. J. Med. Chem.* **2018**, *145*, 649–660 DOI: 10.1016/j.ejmech.2018.01.032.

(109) Li, G.-B.; Abboud, M. I.; Brem, J.; Someya, H.; Lohans, C. T.; Yang, S.-Y.; Spencer, J.; Wareham, D. W.; McDonough, M. A.; Schofield, C. J. NMR-Filtered Virtual Screening Leads to Non-Metal Chelating Metallo-β-Lactamase Inhibitors. *Chem. Sci.* **2017**, *8* (2), 928–937 DOI: 10.1039/c6sc04524c.

(110) Shen, B.; Zhu, C.; Gao, X.; Liu, G.; Song, J.; Yu, Y. Oligopeptides as Full-Length New Delhi Metallo-β-Lactamase-1 (NDM-1) Inhibitors. *PLoS One* **2017**, *12* (5), 1–11 DOI: 10.1371/journal.pone.0177293.

(111) Kosmopoulou, M. . H. P. . S. J. Crystal Structure of the Metallo-Beta-Lactamase NDM-1 in Complex with a Bisthiazolidine Inhibitor. *To Be Publ.* DOI: 10.2210/PDB4U4L/PDB.

(112) González, M. M.; Kosmopoulou, M.; Mojica, M. F.; Castillo, V.; Hinchliffe, P.; Pettinati, I.; Brem, J.; Schofield, C. J.; Mahler, G.; Bonomo, R. A.; et al. Bisthiazolidines: A Substrate-Mimicking Scaffold as an Inhibitor of the NDM-1 Carbapenemase. *ACS Infect. Dis.* **2016**, *1* (11), 544–554 DOI: 10.1021/acsinfecdis.5b00046.

(113) Hinchliffe, P.; González, M. M.; Mojica, M. F.; González, J. M.; Castillo, V.; Saiz, C.; Kosmopoulou, M.; Tooke, C. L.; Llarrull, L. I.; Mahler, G.; et al. Cross-Class Metallo-β-Lactamase Inhibition by Bisthiazolidines Reveals Multiple Binding Modes. *Proc. Natl. Acad. Sci.* **2016**, *113* (26), E3745–E3754 DOI: 10.1073/pnas.1601368113.

(114) Cain, R.; Brem, J.; Zollman, D.; McDonough, M. A.; Johnson, R. M.; Spencer, J.; Makena, A.; Abboud, M. I.; Cahill, S.; Lee, S. Y.; et al. In Silico Fragment-Based Design Identifies Subfamily B1 Metallo-β-Lactamase Inhibitors. *J. Med. Chem.* **2018**, *61* (3), 1255–1260 DOI: 10.1021/acs.jmedchem.7b01728.

(115) Skagseth, S.; Akhter, S.; Paulsen, M. H.; Muhammad, Z.; Lauksund, S.; Samuelsen, Ø.; Leiros, H. K. S.; Bayer, A. Metallo-β-Lactamase Inhibitors by Bioisosteric Replacement: Preparation, Activity and Binding. *Eur. J. Med. Chem.* **2017**, *135*, 159–173 DOI: 10.1016/j.ejmech.2017.04.035.

(116) Song, G. Q.; Wang, W. M.; Li, Z. S.; Wang, Y.; Wang, J. G. First Identification of Isatin-β-Thiosemicarbazones as Novel Inhibitors of New Delhi Metallo-β-Lactamase-1: Chemical Synthesis, Biological Evaluation and Molecular Simulation. *Chinese Chem. Lett.* **2018**, *29* (6), 899–902 DOI: 10.1016/j.cclet.2017.09.035.

(117) Bauer, D. J. Chemoprophylaxis of Smallpox and Treatment of Vaccinia Gangrenosa with 1-Methylisatin 3-Thiosemicarbazone. *Antimicrob. Agents Chemother.* **1965**, *5*, 544–547 DOI: DOI 10.1016/j.patcog.2007.10.002.

(118) Falconer, S. B.; Wang, W.; Gehrke, S. S.; Cuneo, J. D.; Britten, J. F.; Wright, G. D.; Brown, E. D. Metal-Induced Isomerization Yields an Intracellular Chelator That Disrupts Bacterial Iron Homeostasis. *Chem. Biol.* **2014**, *21* (1), 136–145 DOI: 10.1016/j.chembiol.2013.11.007.

(119) Falconer, S. B.; Reid-Yu, S. A.; King, A. M.; Gehrke, S. S.; Wang, W.; Britten, J. F.; Coombes, B. K.; Wright, G. D.; Brown, E. D. Zinc Chelation by a Small-Molecule Adjuvant Potentiates Meropenem Activity in Vivo against NDM-1-Producing Klebsiella Pneumoniae. *ACS Infect. Dis.* **2016**, *1* (11), 533–543 DOI: 10.1021/acsinfecdis.5b00033.

(120) Feng, L.; Yang, K. W.; Zhou, L. S.; Xiao, J. M.; Yang, X.; Zhai, L.; Zhang, Y. L.; Crowder, M. W. N-Heterocyclic Dicarboxylic Acids: Broad-Spectrum Inhibitors of Metallo-β-Lactamases with Co-Antibacterial Effect against Antibiotic-Resistant Bacteria. *Bioorganic Med. Chem. Lett.* **2012**, *22* (16), 5185–5189 DOI: 10.1016/j.bmcl.2012.06.074.

(121) Yang, S.-K.; Kang, J. S.; Oelschlaeger, P.; Yang, K.-W. Azolylthioacetamide: A Highly Promising Scaffold for the Development of Metallo-β-Lactamase Inhibitors. *ACS Med. Chem. Lett.* **2015**, *6* (4), 455–460 DOI: 10.1021/ml500534c.

(122) Zhang, Y. L.; Yang, K. W.; Zhou, Y. J.; LaCuran, A. E.; Oelschlaeger, P.; Crowder, M. W. Diaryl-Substituted Azolylthioacetamides: Inhibitor Discovery of New Delhi Metallo-β-Lactamase-1 (NDM-1). *ChemMedChem* **2014**, *9* (11), 2445–2448 DOI: 10.1002/cmdc.201402249.

(123) Zhai, L.; Zhang, Y. L.; Kang, J. S.; Oelschlaeger, P.; Xiao, L.; Nie, S. S.; Yang, K. W. Triazolylthioacetamide: A Valid Scaffold for the Development of New Delhi Metallo-β-Lactmase-1 (NDM-1) Inhibitors. *ACS Med. Chem. Lett.* **2016**, *7* (4), 413–417 DOI: 10.1021/acsmedchemlett.5b00495.

(124) Xiang, Y.; Chang, Y. N.; Ge, Y.; Kang, J. S.; Zhang, Y. L.; Liu, X. L.; Oelschlaeger, P.; Yang, K. W. Azolylthioacetamides as a Potent Scaffold for the Development of Metallo-β-Lactamase Inhibitors. *Bioorganic Med. Chem. Lett.* **2017**, *27* (23), 5225–5229 DOI: 10.1016/j.bmcl.2017.10.038.

(125) Spyrakis, F.; Celenza, G.; Marcoccia, F.; Santucci, M.; Cross, S.; Bellio, P.; Cendron, L.;

Perilli, M.; Tondi, D. Structure-Based Virtual Screening for the Discovery of Novel Inhibitors of New Delhi Metallo-β-Lactamase-1. *ACS Med. Chem. Lett.* **2018**, 45–50 DOI: 10.1021/acsmedchemlett.7b00428.

(126) Wang, X.; Lu, M.; Shi, Y.; Ou, Y.; Cheng, X. Discovery of Novel New Delhi Metallo-β-Lactamases-1 Inhibitors by Multistep Virtual Screening. *PLoS One* **2015**, *10* (3), 1–17 DOI: 10.1371/journal.pone.0118290.

(127) Hassan, M.; Thakur, P.; Kumar, J.; Ray, D.; Anjum, F. Search of Potential Inhibitor against New Delhi Metallo-Beta-Lactamase 1 from a Series of Antibacterial Natural Compounds. *J. Nat. Sci. Biol. Med.* **2013**, *4* (1), 51 DOI: 10.4103/0976-9668.107260.

(128) Grant, E. B.; Guiadeen, D.; Baum, E. Z.; Foleno, B. D.; Jin, H.; Montenegro, D. A.; Nelson, E. A.; Bush, K.; Hlasta, D. J. The Synthesis and SAR of Rhodanines as Novel Class C β-Lactamase Inhibitors. *Bioorganic Med. Chem. Lett.* **2000**, *10* (19), 2179–2182 DOI: 10.1016/S0960-894X(00)00444-3.

(129) Zervosen, A.; Lu, W. P.; Chen, Z.; White, R. E.; Demuth, T. P.; Frère, J. M. Interactions between Penicillin-Binding Proteins (PBPs) and Two Novel Classes of PBP Inhibitors, Arylalkylidene Rhodanines and Arylalkylidene Iminothiazolidin-4-Ones. *Antimicrob. Agents Chemother.* **2004**, *48* (3), 961–969 DOI: 10.1128/AAC.48.3.961-969.2004.

(130) Spicer, T.; Minond, D.; Enogieru, I.; Saldanha, S. A.; Allais, C.; Liu, Q.; Mercer, B. A.; Roush, W. R.; Hodder, P. ML302, a Novel β-Lactamase (BLA) Inhibitor. In *Probe Reports from the NIH Molecular Libraries Program*; Bethesda (MD), 2010.

(131) Xiang, Y.; Chen, C.; Wang, W.-M.; Xu, L.-W.; Yang, K.-W.; Oelschlaeger, P.; He, Y. Rhodanine as a Potent Scaffold for the Development of Broad-Spectrum Metallo-β-Lactamase Inhibitors. *ACS Med. Chem. Lett.* **2018**, *9* (4), 359–364 DOI: 10.1021/acsmedchemlett.7b00548.

(132) Brem, J.; Van Berkel, S. S.; Aik, W.; Rydzik, A. M.; Avison, M. B.; Pettinati, I.; Umland, K. D.; Kawamura, A.; Spencer, J.; Claridge, T. D. W.; et al. Rhodanine Hydrolysis Leads to Potent Thioenolate Mediated Metallo-β 2-Lactamase Inhibition. *Nat. Chem.* **2014**, *6* (12), 1084–1090 DOI: 10.1038/nchem.2110.

(133) Chen, A. Y.; Thomas, P. W.; Stewart, A. C.; Bergstrom, A.; Cheng, Z.; Miller, C.; Bethel, C. R.; Marshall, S. H.; Credille, C. V.; Riley, C. L.; et al. Dipicolinic Acid Derivatives as Inhibitors of New Delhi Metallo-β-Lactamase-1. *J. Med. Chem.* **2017**, *60* (17), 7267–7283 DOI: 10.1021/acs.jmedchem.7b00407.

(134) Hinchliffe, P.; Tanner, C. A.; Krismanich, A. P.; Labbé, G.; Goodfellow, V. J.; Marrone, L.; Desoky, A. Y.; Calvopiña, K.; Whittle, E. E.; Zeng, F.; et al. Structural and Kinetic Studies

of the Potent Inhibition of Metallo-β-Lactamases by 6-Phosphonomethylpyridine-2-Carboxylates. *Biochemistry* **2018**, *57* (12), 1880–1892 DOI: 10.1021/acs.biochem.7b01299.

(135) Jacobsen, J. A.; Major Jourden, J. L.; Miller, M. T.; Cohen, S. M. To Bind Zinc or Not to Bind Zinc: An Examination of Innovative Approaches to Improved Metalloproteinase Inhibition. *Biochim. Biophys. Acta - Mol. Cell Res.* **2010**, *1803* (1), 72–94 DOI: 10.1016/j.bbamcr.2009.08.006.

(136) Chen, C. C. H.; Rahil, J.; Pratt, R. F.; Herzberg, O. Structure of a Phosphonate-Inhibited β-Lactamase: An Analog of the Tetrahedral Transition State/Intermediate of β-Lactam Hydrolysis. *J. Mol. Biol.* **1993**, *234* (1), 165–178 DOI: 10.1006/jmbi.1993.1571.

(137) Hecker, S. J.; Reddy, K. R.; Totrov, M.; Hirst, G. C.; Lomovskaya, O.; Griffith, D. C.; King, P.; Tsivkovski, R.; Sun, D.; Sabet, M.; et al. Discovery of a Cyclic Boronic Acid β-Lactamase Inhibitor (RPX7009) with Utility vs Class A Serine Carbapenemases. *J. Med. Chem.* **2015**, *58* (9), 3682–3692 DOI: 10.1021/acs.jmedchem.5b00127.

(138) Zhou, M.; Yang, Q.; Lomovskaya, O.; Sun, D.; Kudinha, T.; Xu, Z.; Zhang, G.; Chen, X.; Xu, Y. In Vitro Activity of Meropenem Combined with Vaborbactam against KPC-Producing Enterobacteriaceae in China. *J. Antimicrob. Chemother.* **2018**, *73* (10), 2789–2796 DOI: 10.1093/jac/dky251.

(139) Brem, J.; Cain, R.; Cahill, S.; McDonough, M. A.; Clifton, I. J.; Jiménez-Castellanos, J.-C.; Avison, M. B.; Spencer, J.; Fishwick, C. W. G.; Schofield, C. J. Structural Basis of Metallo-β-Lactamase, Serine-β-Lactamase and Penicillin-Binding Protein Inhibition by Cyclic Boronates. *Nat. Commun.* **2016**, *7* DOI: 10.1038/ncomms12406.

(140) Powers, R. A.; Blázquez, J.; Weston, G. S.; Morosini, M. I.; Baquero, F.; Shoichet, B. K. The Complexed Structure and Antimicrobial Activity of a Non-β-Lactam Inhibitor of AmpC β-Lactamase. *Protein Sci.* **1999**, *8* (11), 2330–2337 DOI: 10.1110/ps.8.11.2330.

(141) Venturelli, A.; Tondi, D.; Cancian, L.; Morandi, F.; Cannazza, G.; Segatore, B.; Prati, F.; Amicosante, G.; Shoichet, B. K.; Costi, M. P. Optimizing Cell Permeation of an Antibiotic Resistance Inhibitor for Improved Efficacy. *J. Med. Chem.* **2007**, *50* (23), 5644–5654 DOI: 10.1021/jm070643q.

(142) Santucci, M.; Spyrakis, F.; Cross, S.; Quotadamo, A.; Farina, D.; Tondi, D.; De Luca, F.; Docquier, J. D.; Prieto, A. I.; Ibacache, C.; et al. Computational and Biological Profile of Boronic Acids for the Detection of Bacterial Serine- and Metallo-β-Lactamases. *Sci. Rep.* **2017**, *7* (1), 1–15 DOI: 10.1038/s41598-017-17399-7.

(143) Mercuri, P. S.; García-Sáez, I.; De Vriendt, K.; Thamm, I.; Devreese, B.; Van Beeumen, J.; Dideberg, O.; Rossolini, G. M.; Frère, J. M.; Galleni, M. Probing the Specificity of the

Subclass B3 FEZ-1 Metallo-β-Lactamase by Site-Directed Mutagenesis. *J. Biol. Chem.* **2004**, *279* (32), 33630–33638 DOI: 10.1074/jbc.M403671200.

(144) Thomas, P. W.; Cammarata, M.; Brodbelt, J. S.; Fast, W. Covalent Inhibition of New Delhi Metallo-β-Lactamase-1 (NDM-1) by Cefaclor. *ChemBioChem* **2014**, *15* (17), 2541–2548 DOI: 10.1002/cbic.201402268.

(145) Parnham, M. J.; Sies, H. The Early Research and Development of Ebselen. *Biochem. Pharmacol.* **2013**, *86* (9), 1248–1253 DOI: 10.1016/j.bcp.2013.08.028.

(146) Chiou, J.; Wan, S.; Chan, K. F.; So, P. K.; He, D.; Chan, E. W. C.; Chan, T. H.; Wong, K. Y.; Tao, J.; Chen, S. Ebselen as a Potent Covalent Inhibitor of New Delhi Metallo-β-Lactamase (NDM-1). *Chem. Commun.* **2015**, *51* (46), 9543–9546 DOI: 10.1039/c5cc02594j.

(147) Jin, W. Bin; Xu, C.; Cheng, Q.; Qi, X. L.; Gao, W.; Zheng, Z.; Chan, E. W. C.; Leung, Y. C.; Chan, T. H.; Wong, K. Y.; et al. Investigation of Synergistic Antimicrobial Effects of the Drug Combinations of Meropenem and 1,2-Benzisoselenazol-3(2H)-One Derivatives on Carbapenem-Resistant Enterobacteriaceae Producing NDM-1. *Eur. J. Med. Chem.* **2018**, *155*, 285–302 DOI: 10.1016/j.ejmech.2018.06.007.

(148) Christopeit, T.; Leiros, H. K. S. Fragment-Based Discovery of Inhibitor Scaffolds Targeting the Metallo-β-Lactamases NDM-1 and VIM-2. *Bioorganic Med. Chem. Lett.* **2016**, *26* (8), 1973–1977 DOI: 10.1016/j.bmcl.2016.03.004.

(149) Christopeit, T.; Albert, A.; Leiros, H. K. S. Discovery of a Novel Covalent Non-β-Lactam Inhibitor of the Metallo-β-Lactamase NDM-1. *Bioorganic Med. Chem.* **2016**, *24* (13), 2947–2953 DOI: 10.1016/j.bmc.2016.04.064.

(150) Thomas, P. W.; Spicer, T.; Cammarata, M.; Brodbelt, J. S.; Hodder, P.; Fast, W. An Altered Zinc-Binding Site Confers Resistance to a Covalent Inactivator of New Delhi Metallo-β-Lactamase-1 (NDM-1) Discovered by High-Throughput Screening. *Bioorganic Med. Chem.* **2013**, *21* (11), 3138–3146 DOI: 10.1016/j.bmc.2013.03.031.

(151) Shen, B.; Yu, Y.; Chen, H.; Cao, X.; Lao, X.; Fang, Y.; Shi, Y.; Chen, J.; Zheng, H. Inhibitor Discovery of Full-Length New Delhi Metallo-β-Lactamase-1 (NDM-1). *PLoS One* **2013**, *8* (5), 4–10 DOI: 10.1371/journal.pone.0062955.

(152) Rogers, S. A.; Huigens, R. W.; Cavanagh, J.; Melander, C. Synergistic Effects between Conventional Antibiotics and 2-Aminoimidazole-Derived Antibiofilm Agents. *Antimicrob. Agents Chemother.* **2010**, *54* (5), 2112–2118 DOI: 10.1128/AAC.01418-09.

(153) Worthington, R. J.; Bunders, C. A.; Reed, C. S.; Melander, C. Small Molecule Suppression of Carbapenem Resistance in NDM-1 Producing Klebsiella Pneumonia. *Acs Med. Chem. Lett.* **2012**, *3*, 1–74 DOI: 10.1021/ml200290p.

(154) Everett, M.; Sprynski, N.; Coelho, A.; Castandet, J.; Bayet, M.; Bougnon, J.; Lozano, C.; Davies, D. T.; Leiris, S.; Zalacain, M.; et al. Discovery of a Novel Metallo-β-Lactamase Inhibitor That Potentiates Meropenem Activity against Carbapenem-Resistant Enterobacteriaceae. *Antimicrob. Agents Chemother.* **2018**, *62* (5) DOI: 10.1128/AAC.00074-18.

(155) Liu, S.; Zhou, Y.; Niu, X.; Wang, T.; Li, J.; Liu, Z.; Wang, J.; Tang, S.; Wang, Y.; Deng, X. Magnolol Restores the Activity of Meropenem against NDM-1-Producing Escherichia Coli by Inhibiting the Activity of Metallo-β-Lactamase. *Cell Death Discov.* **2018**, *4* (1), 28 DOI: 10.1038/s41420-018-0029-6.

(156) González, L. J.; Bahr, G.; Nakashige, T. G.; Nolan, E. M.; Bonomo, R. A.; Vila, A. J. Membrane Anchoring Stabilizes and Favors Secretion of New Delhi Metallo-β-Lactamase. *Nat. Chem. Biol.* **2016**, *12*, 516.

(157) Castanheira, M.; Rhomberg, P. R.; Flamm, R. K.; Jones, R. N. Effect of the β-Lactamase Inhibitor Vaborbactam Combined with Meropenem against Serine Carbapenemase-Producing Enterobacteriaceae. *Antimicrob. Agents Chemother.* **2016**, *60* (9), 5454–5458 DOI: 10.1128/AAC.00711-16.

For Table of Contents Use Only

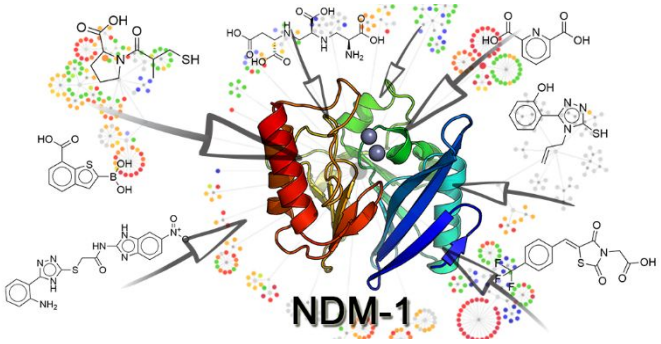

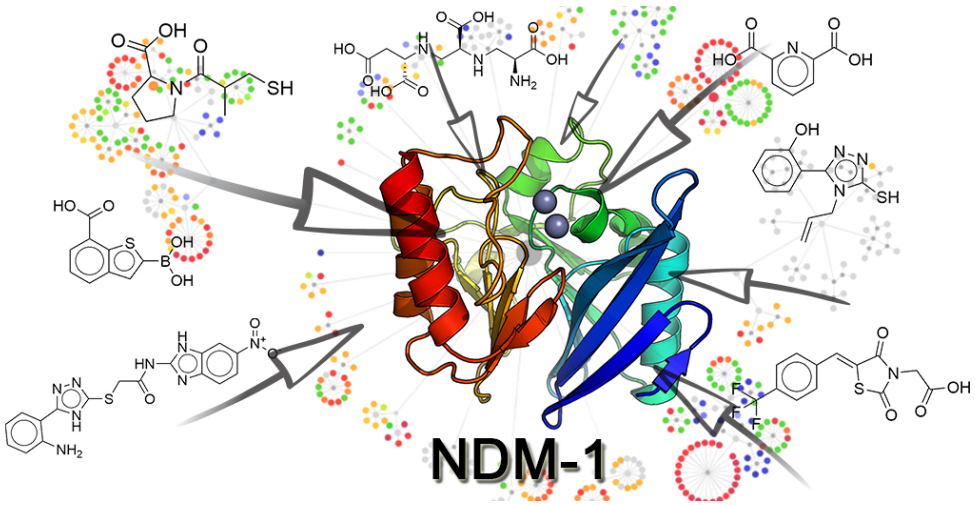

Table of contents

88x44mm (300 x 300 DPI)